3304 *Organometallics* **1993,** *12,* 3304-3315

(η^5-Benzyl)manganese Complexes. 2. Preparation, Characterization, and Reactivity of [η^5-$C_6Me_5(CH_2)$]$Mn(CO)_2PR_3$ (R = *n*-Bu, Me, Ph, OMe, OPh). Structure of [η^5-$C_6Me_5(CH_2)$]$Mn(CO)_2PMe_3$

Jeffrey L. Moler,[1] Darrell P. Eyman,* Joy M. Nielson, Ann M. Morken,
Steven J. Schauer, and Daniel B. Snyder

Department of Chemistry, University of Iowa, Iowa City, Iowa 52242

Received January 29, 1993

A series of (η^5-pentamethylbenzyl)$Mn(CO)_2PR_3$ complexes has been synthesized (η^5-pentamethylbenzyl = η^5-pentamethylcyclohexadienyl-*exo*-ene). Phosphine ligand substitution increases the electron density on the manganese and enhances the nucleophilicity of the exocyclic methylene. Nucleophilic reactions have been observed to form C–C bonds with CH_3I and PhC(O)Cl and C–I bonds with I_2. The [η^5-$C_6Me_5(CH_2)$]$Mn(CO)_2PMe_3$ (**2b**) complex reacts with $Mn(CO)_5Br$ and (η^5-C_5H_5)$Fe(CO)_2I$ to displace halide and form bimetallic species, isolated as {[η^6-$C_6Me_5(CH_2Mn(CO)_5)$]$Mn(CO)_2PMe_3$}PF_6 and {[η^6-$C_6Me_5(CH_2Fe(Cp)(CO)_2)$]$Mn(CO)_2PMe_3$}I. The benzyls also react by a radical pathway with the halocarbons CCl_4, $CDCl_3$, and $CHBr_3$, to form a new C–C bond at the exocyclic methylene. ESR studies support a proposed radical mechanism in the reactions of [η^5-$C_6Me_5(CH_2)$]$Mn(CO)_2L$ (L = CO (**2**), P(n-Bu)$_3$ (**2a**), PMe_3 (**2b**)) with CCl_4. ESR measurements of reaction mixtures provided a g_{iso} value of 2.192(3) (**2**, **2a**, **2b**). The solid-state structure of **2b** confirms the pentahapticity and the uncoordinated exocyclic double bond in the η^5-cyclohexadienyl ligand. Complex **2b** crystallizes in the monoclinic space group $P2_1/c$ with cell dimensions a = 11.967(4) Å, b = 10.093(6) Å, c = 15.232(4) Å, β = 102.70(5)°, V = 1795(1) Å^3, Z = 4, R_1 = 0.059, R_2 = 0.078, and ρ_{calcd} = 1.556 Mg·m^{-3}.

Introduction

Hydrocarbon C–H bonds have been activated using three systematic approaches. They can be oxidized by a radical mechanism,[2] eq 1, or reduced by oxidative addition to

$$R^{\bullet} + O_2 \rightarrow ROO^{\bullet} \xrightarrow{RH} ROOH + R^{\bullet} \qquad (1)$$

$$R\text{–}H + M \rightarrow R\text{–}M\text{–}H \qquad (2)$$

$$MRH + O_2 \rightarrow MRH^+O_2^- \xrightarrow{-HO_2} MR \qquad (3)$$

$$[(\eta^6\text{-}C_6Me_6)Mn(CO)_3]^+ + KH \xrightarrow{-H_2} [\eta^5\text{-}C_6Me_5(CH_2)]Mn(CO)_3 \qquad (4)$$

transition metals, eq 2.[3] Astruc has developed a third route in which initiation occurs by a single electron transfer to O_2 from an organoiron complex, eq 3.[4] A methyl group of the coordinated hexamethylbenzene ligand in the intermediary CpFe(η^6-C_6Me_6)$^+O_2^{\bullet-}$ complex is subsequently deprotonated by $O_2^{\bullet-}$. Astruc also has formed the activated complex, CpFe[η^5-$C_6Me_5(CH_2)$], by deprotonation of methyl substituents of the arene in CpFe(η^6-C_6Me_6) using KO_2 and t-BuOK.[4d] We have reported similar observations for the (arene)manganese complex [(η^6-C_6Me_6)$Mn(CO)_3$]PF_6 (**1**).[5] In our experiments, a methyl of the hexamethylbenzene ligand of **1** is depronated using KH, or other strong bases, to form [η^5-$C_6Me_5(CH_2)$]$Mn(CO)_3$ (**2**), eq 4. Gladfelter confirmed and extended this chemistry to other (η^6-arene)manganese tricarbonyl complexes.[6] The activated complexes generated by each of these methods can undergo a variety of reactions leading to the formation of new C–C bonds and carbon bonds to other elements.

The exocyclic methylene on the metal-coordinated η^5-cyclohexadienyl-*exo*-ene ligand, (η^5-pentamethylbenzyl), can undergo nucleophilic, radical, and other reactions to form C–C, C–I, C–Mn, C–Fe, and C–H bonds. Astruc et al. extensively investigated the reactivity of the CpFe(η^5-pentamethylbenzyl) (**3**) complex with a variety of electrophiles.[4,7] Reactivity of the exocyclic methylene provided an efficient means of alkylating and functionalizing the methyl groups in the CpFe(arene) complex.[8] Similar reactions for **2** have been reported by our laboratory.[5]

---

[1] Air University, Air Force Institute of Technology (AFIT/CIRD), Wright-Patterson AFB, Dayton, OH 45433-6583 (Department of Chemistry, University of Iowa, Iowa City, IA).

[2] (a) Davies, A. G. *J. Organomet. Chem.* **1980,** *200,* 87–99. (b) Mayo, F. R. *Acc. Chem. Res.* **1968,** *1,* 193–201.

[3] (a) Kochi, J. K. *Organometallic Mechanism and Catalysis*; Academic Press: New York, 1978; pp 517–522. (b) Stille, J. K.; Lau, K. S. Y. *Acc. Chem. Res.* **1977,** *10,* 434–442. (c) Osborn, J. A. In *Organotransition Metal Chemistry*; Ishii, I., Tsutsui, M., Eds.; Plenum Press: New York, 1975; pp 65–80. (d) Halpern, J. *Acc. Chem. Res.* **1970,** *3,* 386–392. (e) Collman, J. P. *Acc. Chem. Res.* **1968,** *1,* 136–143. (f) Collman, J. P.; Roper, W. R. *Adv. Organomet. Chem.* **1968,** *7,* 53–94.

[4] (a) Astruc, D. In *The Chemistry of the Metal-Carbon Bond*; Hartley, F. R., Patai, S., Eds.; Wiley: New York, 1987; Vol, 4, pp 625–731. (b) Hamon, J.-R.; Astruc, D. *Organometallics* **1988,** *7,* 1036–1046. (c) Madonik, A. M.; Astruc, D. *J. Am. Chem. Soc.* **1984,** *106,* 2437–2439. (d) Astruc, D.; Hamon, J.-R.; Román, E.; Michaud, P. *J. Am. Chem. Soc.* **1981,** *103,* 7502–7514. (e) Hamon, J.-R.; Astruc, D.; Román, E.; Batail, P.; Mayerle, J. J. *J. Am. Chem. Soc.* **1981,** *103,* 2431–2433. (f) Astruc, D.; Román, E.; Hamon, J.-R.; Batail, P. *J. Am. Chem. Soc.* **1979,** *101,* 2240–2242.

[5] LaBrush, D. M.; Eyman, D. P.; Baenziger, N. C.; Mallis, L. M. *Organometallics* **1991,** *10,* 1026–1033.

[6] Hull, J. W., Jr.; Roesselet, K. J.; Galdfelter, W. L. *Organometallics* **1992,** *11,* 3630–3635.

0276-7333/93/2312-3304$04.00/0

Although **2** undergoes many of the same nucleophilic and radical substitution reactions as **3** at the exocyclic methylene, it is less nucleophilic.[5] Apparently, the carbonyl ligands in **2** contribute less electron density to the metal and therefore decrease reactivity at the exocyclic methylene. Astruc reported the formation of several stable bimetallic complexes resulting from the reaction of **3** with transition metal halides.[4d] Complex **2** is not sufficiently nucleophilic to displace halide from organotransition metal halide complexes, including $Mn(CO)_5Br$ and $(\eta^5\text{-}C_5H_5)Fe(CO)_2Cl$.[5] The reactivity of **2** might be anticipated to be enhanced by increasing the electron density on the metal. This can be accomplished by selective ligand substitution, for example, replacement of one carbonyl on the manganese with a stronger σ-donor ligand such as alkyl- and aryl-substituted phosphines and phosphites.[9] Alkyl- and aryl-substituted phosphites are good σ-donors but have greater π-back-bonding capability. This places the electron-donor ability of the phosphite ligand between that of the phosphines and carbonyl ligands. Increased σ-donation to the manganese should increase the electron density at the exocyclic methylene, thus enhancing its reactivity. We have reported that hydride transfer from *endo*-$(\eta^5\text{-}C_6Me_6H)Mn(CO)_2PR_3$ is directly affected by the σ-donor ability of the phosphine substituent.[10] Substitution of cyanide, a very strong σ-donor, for carbonyl allows the formation of $\{[\eta^5\text{-}C_6Me_5(CH_2)]Mn(CO)_2CN\}^-$, which is strongly nucleophilic at the exocyclic methylene.[11]

We report here the preparation and reactivity of $[\eta^5\text{-}C_6Me_5(CH_2)]Mn(CO)_2PR_3$ (R = *n*-Bu (**2a**), Me (**2b**), Ph (**2c**), OMe (**2d**), OPh (**2e**)). It will be shown that phosphine ligand substitution for CO increases the nucleophilic reactivity of the exocyclic methylene over that observed for **2**. The solid-state structure of **2b** demonstrates that phosphine substitution for a carbonyl in **2** does not significantly alter the π-carbocyclic system of the η^5-pentamethylbenzyl ligand. The effect of enhanced nucleophilicity at the exocyclic methylene may arise through an electronic transmission other than through the π-carbocyclic system.

Experimental Section

Reactions and recrystallizations were performed under dinitrogen or argon using either standard Schlenk or glovebox techniques.[12] Solvents were dried over suitable reagents and freshly distilled under dinitrogen.[13] Solvents were further deoxygenated prior to use by multiple freeze–pump–thaw cycles or by bubbling dinitrogen or argon through the liquid. Untreated silica gel (60–200 mesh) was used for liquid chromatographic separations (LC).

Infrared spectra were obtained on a Mattson Cygnus 25 FTIR spectrometer, using 0.5-mm KBr cells or KBr mull and press techniques. ^1H, ^2H, ^{13}C, $^{13}C\{^1H\}$, and $^{31}P\{^1H\}$ NMR spectra were recorded on either a Bruker AC300 or WM360 spectrometer. The ^1H, ^2H, and ^{13}C NMR shifts are reported with respect to Me_4Si (δ 0.0 ppm). $^{31}P\{^1H\}$ NMR shifts are reported with respect to an external standard, H_3PO_4 (85%) (δ 0.0 ppm). All downfield chemical shifts are positive. ESR spectra were obtained using a Varian E-104 X-band spectrometer at liquid nitrogen temperatures. High resolution accurate mass measurements were obtained using a VG ZAB-HF mass spectrometer in the FAB ionization mode at the University of Iowa Mass Spectrometry Center or at the Midwest Center for Mass Spectrometry. Elemental analyses were obtained from Desert Analytics. Compounds **2a–e**, **9**, and **10** were not stable enough to be sent out for elemental analysis.

Cyclic voltammograms were obtained, under inert-atmospheric conditions, using a three-electrode system consisting of a 6.28-mm² Pt disk working electrode, a coiled Pt wire counter electrode, and a Ag|AgCl reference electrode. The supporting electrolyte for the reference electrode was a LiCl saturated, 0.1 M $(n\text{-}Bu)_4NBF_4$ THF solution. The reference electrode was suspended within a Luggin capillary to minimize the *iR* drop across the electrodes. Electrochemistry was carried out with a PAR 173 potentiostat in conjunction with a PAR 175 programmer. Cyclic voltammograms, recorded using a HP 7040A X-Y recorder, were corrected using ferrocene versus the Ag|AgCl reference electrode ($E_p = +0.342$ V) and a standard calcium chloride calomel electrode (SCE) ($E_p = +0.630$ V).

Syntheses. The $[(\eta^6\text{-}C_6Me_6)Mn(CO)_2PR_3]PF_6$ complexes (R = *n*-Bu (**1a**), Me (**1b**), Ph (**1c**), OMe (**1d**), and OPh (**1e**)) were prepared by published methods.[10]

$[\eta^5\text{-}C_6Me_5(CH_2)]Mn(CO)_2PMe_3$ (2b). Procedure a. A tetrahydrofuran solution (30 mL) of **1b** (172 mg, 348 μmol) was added to an excess of dry KH (>50 equiv) with stirring. Immediately, the color of the solution turned from pale to golden yellow. After 15 min, the solution was decanted and the solvent removed under reduced pressure. Hexane was used to extract the product. The procedure was repeated producing yellow-orange crystals of **2b** in nearly quantitative yield. Compound **2b** was purified by sublimation at 65–70 °C, providing orange crystals. Yield: 118 mg (97%). IR (THF): ν_{CO} 1924, 1858 cm^{-1}. ^1H NMR (C_6D_6): δ 3.60 (d, 2 H, $=CH_2$, $^2J_{P-H} = 1.4$ Hz), 2.02 (s, 3 H, $-CH_3$), 1.87 (s, 6 H, $-CH_3$), 1.56 (s, 6 H, $-CH_3$), 1.15 (d, 9 H, $P(CH_3)_3$, $^2J_{P-H} = 10.1$ Hz). $^{13}C\{^1H\}$ NMR (C_6D_6): δ 233.0 (CO), 146.4 ($C{=}CH_2$), 108.4, 78.8 (ring C), 77.2 ($=CH_2$), 19.2 ($P(CH_3)_3$), 18.0, 17.7–17.1, 16.2 ($-CH_3$). $^{31}P\{^1H\}$ NMR (C_6D_6): δ 21.3 (s, PMe_3). MW_{calc} [M^+] 348.1051; M^+_{exp} m/z 348.1062 ($\Delta m = +1.1$ mmu).

Procedure b. A tetrahydrofuran solution (100 mL) of **1b** (250 mg, 505 μmol), when injected with 1.1 equiv of either methyllithium or *tert*-butyllithium, turned from a light yellow to golden-yellow color. Carbonyl stretching frequencies indicate that not all **1b** is converted to **2b**. IR (THF): 1970, 1924, 1858 cm^{-1}.

Procedure c. A slurry of NaOH in tetrahydrofuran added to **1b** (125 mg, 252 μmol) produced a golden-yellow mixture of **1b** and **2b**. IR (THF): 1970, 1924, 1858 cm^{-1}.

$[\eta^5\text{-}C_6Me_5(CH_2)]Mn(CO)_2P(n\text{-}Bu)_3$ (2a). Procedure a. Compound **1a** (154 mg, 248 μmol) was used to produce **2a** as orange crystals. Yield: 114 mg (97%). IR (THF): ν_{CO} 1920, 1859 cm^{-1}. ^1H NMR (C_6D_6): δ 3.63 (d, 2 H, $=CH_2$, $^2J_{P-H} = 1.2$ Hz), 2.07 (s, 3 H, $-CH_3$), 1.91 (s, 6 H, $-CH_3$), 1.69 (s, 6 H, $-CH_3$), 1.43 (m, 12 H, $P(-CH_2-)_2$), 1.31 (m, 6 H, $P(CH_2-)$), 0.89 (t, 9 H, $P(-CH_3)$, $^3J_{H-H} = 7.2$ Hz). $^{13}C\{^1H\}$ NMR (C_6D_6): δ 228.7 (CO, $^2J_{P-C} = 21.8$ Hz), 145.5 ($C{=}CH_2$), 108.0, 87.3 (ring C), 79.6

---

(7) (a) Astruc, D.; Mandon, D.; Madonik, A.; Michaud, P.; Ardoin, N.; Varret, F. *Organometallics* **1990**, *9*, 2155–2164. (b) Mandon, D.; Astruc, D. *Organometallics* **1990**, *9*, 341–346. (c) Astruc, D.; Hamon, J.-R.; Lacoste, M.; Desbois, M.-H.; Madonik, A. M.; Román, E. *Organomet. Synth.* **1988**, *4*, 172. (d) Mandon, D.; Astruc, D. *J. Organomet. Chem.* **1986**, *307*, C27–C30. (e) Astruc, D. *Acc. Chem. Res.* **1986**, *19*, 377–383. (f) Madonik, A. M.; Mandon, D.; Michaud, P.; Lapinte, C.; Astruc, D. *J. Am. Chem. Soc.* **1984**, *106*, 3381–3382. (g) Catheline, D.; Astruc, D. *Organometallics* **1984**, *3*, 1094–1100. (h) Madonik, A. M.; Astruc, D. *J. Am. Chem. Soc.* **1984**, *106*, 2437–2439. (i) Hamon, J.-R.; Astruc, D. *J. Am. Chem. Soc.* **1983**, *105*, 5951–5952.

(8) (a) Moriarty, R. M.; Gill, U. S. *Organometallics* **1986**, *5*, 253–256. (b) Gill, U. S.; Moriarty, R. M. *Synth. React. Inorg. Met.-Org. Chem.* **1986**, *16*, 485–490. (c) Lee, C. C.; Abd-El Aziz, A. S.; Chowdhurry, R. L.; Gill, U. S.; Piorko, A.; Sutherland, R. G. *J. Organomet. Chem.* **1986**, *315*, 79–92. (d) Khand, I. U.; Paulson, P. L.; Watts, W. E. *J. Chem. Soc. C* **1969**, 2024–2033.

(9) Tolman, C. A. *Chem. Rev.* **1977**, *77*, 313–348.

(10) Snyder, D. B.; Schauer, S. J.; Eyman, D. P.; Moler, J. L.; Weers, J. J. Submitted for publication in *J. Am. Chem. Soc.*

(11) Morken, A. M.; Eyman, D. P. Unpublished results, The University of Iowa.

(12) Shriver, D. F.; Drezdon, M. A. *The Manipulation of Air Sensitive Compounds*; Wiley: New York, 1986.

(13) Perrin, D. D.; Armarego, W. L. F. *Purification of Laboratory Chemicals*, 3rd ed.; Pergamon Press: Oxford, U.K., 1988.

($=CH_2$), 27.3–24.3, 19.9–18.5, 14.8–12.0 ($P(CH_2)_3CH_3$), 17.9–15.7 ($-CH_3$). $^{31}P\{^1H\}$ NMR (C_6D_6): δ 57.2 (s, PBu_3). MW_{calc} [M^+] 474.2459; M^+_{exp} m/z 474.2456 (Δm = −0.4 mmu).

$[\eta^5\text{-}C_6Me_5(CH_2)]Mn(CO)_2PPh_3$ (2c). Procedure a. Compound **1c** (156 mg, 229 μmol) was used to produce **2c** as orange crystals. Yield: 113 mg (92%). IR (THF): ν_{CO} 1927, 1864 cm^{-1}. ^1H NMR (C_6D_6): δ 7.73–7.38 (m, 15 H, $P(C_6H_5)_3$), 3.61 (s, 2 H, $=CH_2$), 1.98 (s, 3 H, $-CH_3$), 1.70 (s, 6 H, $-CH_3$), 1.32 (s, 6 H, $-CH_3$). $^{13}C\{^1H\}$ NMR (C_6D_6): δ 228.8 (CO), 145.0 ($C{=}CH_2$), 134.1–129.3 ($-C_6H_5$), 106.4, 81.8 (ring C), 79.6 ($=CH_2$), 17.1–16.3 ($-CH_3$). $^{31}P\{^1H\}$ NMR (C_6D_6): δ 83.0 (s, PPh_3). MW_{calc} [PPh_3] 262.0911, [$(C_6Me_5CH_2)Mn$] 216.0711, [$C_6Me_5CH_2$] 161.1330; M^+_{exp} m/z 262.0912 (Δm = +0.1 mmu), 216.0682 (Δm = −2.8 mmu), 161.1334 (Δm = +0.4 mmu).

$[\eta^5\text{-}C_6Me_5(CH_2)]Mn(CO)_2P(OMe)_3$ (2d). Procedure a. Compound **1d** (303 mg, 559 μmol) was used to produce **2d** as orange-yellow crystals. Yield: 217 mg (98%). IR (THF): ν_{CO} 1939, 1877 cm^{-1}. ^1H NMR (C_6D_6): δ 3.95 (s, 2 H, $=CH_2$), 3.26 (d, 9 H, $-OCH_3$, $^3J_{P-H}$ = 10.8 Hz), 2.01 (s, 3 H, $-CH_3$), 1.87 (s, 6 H, $-CH_3$), 1.83 (s, 6 H, $-CH_3$). $^{13}C\{^1H\}$ NMR (C_6D_6): δ 230.3 (CO), 148.0 ($C{=}CH_2$), 107.9, 86.6, 80.3 (ring C), 76.9 ($=CH_2$), 51.9 (d, $P(OCH_3)_3$, J_{P-C} = 5.1 Hz), 17.9, 16.8, 15.8 ($-CH_3$). ^{13}C NMR (C_6D_6): δ 76.9 (t, $=CH_2$, J_{C-H} = 156.5 Hz). $^{31}P\{^1H\}$ NMR (C_6D_6): δ 196.4 (s, $P(OMe)_3$). MW_{calc} [M^+] 396.0898; M^+_{exp} m/z 396.0922 (Δm = +2.4 mmu).

$[\eta^5\text{-}C_6Me_5(CH_2)]Mn(CO)_2P(OPh)_3$ (2e). Procedure a. Compound **1e** (301 mg, 413 μmol) was used to produce **2e** as yellow-orange crystals. Yield: 231 mg (96%). IR (THF): ν_{CO} 1955, 1893 cm^{-1}. ^1H NMR (C_6D_6): δ 7.63–7.39 (m, 15 H, $P(OC_6H_5)_3$), 3.28 (s, 2 H, $=CH_2$), 2.00 (s, 3 H, $-CH_3$), 1.86 (s, 6 H, $-CH_3$), 1.82 (s, 6 H, $-CH_3$). $^{13}C\{^1H\}$ NMR (C_6D_6): δ 227.9 (d, CO, $^2J_{P-C}$ = 27 Hz), 152.5 ($C{=}CH_2$), 147.1, 129.8–121.4 ($P(OC_6H_5)_3$), 107.5, 86.6, 84.9, 82.7 (ring C), 77.4 ($=CH_2$), 17.7, 16.7, 15.3 ($-CH_3$). $^{31}P\{^1H\}$ NMR (C_6D_6): δ 170.0 (s, $P(OPh)_3$). MW_{calc} [M^+] 582.1368; M^+_{exp} m/z 582.1345 (Δm = −2.3 mmu).

General Procedure for the Reactions of NH_4PF_6 with Complexes 2a–e. The benzyl complex (**2a–e**, ~250 μmol) was mixed with 1.1 equiv of NH_4PF_6 in ~15 mL of dry THF. An immediate color change from the orange-yellow of the benzyl **2a–e** to the yellow of the cationic species **1a–e** was observed. Complete conversion was verified by the presence of only the ν_{CO} of complexes **1a–e** in the IR spectra, which have been previously reported.[10,14] Recoverable yields were greater than 85% for **1a–e**.

General Procedure for the Reactions of PhC(O)Cl with Complexes 2a–e. A 50-mL THF solution of a benzyl complex (**2a–e**, 150–300 μmol) was injected with 3 equiv of benzoyl chloride and stirred for ~5 min. An immediate color change from yellow-orange to yellow was observed. Verification of complete reaction was obtained by observing the IR ν_{CO} shift to the higher frequencies of the cationic species. The Cl^- anion was metathesized with 1.1 equiv of NH_4PF_6 for **4a–c**. The product was purified by LC on SiO_2 (hexanes–acetone). Spectroscopic characterizations for the previously unreported compounds follow.

$\{[\eta^6\text{-}C_6Me_5(CH_2C(O)Ph)]Mn(CO)_2P(n\text{-}Bu)_3\}PF_6$ (4a): yellow powder; yield, 136 mg (99%); IR (CH_2Cl_2) ν_{CO} 1979, 1932 cm^{-1}, $\nu_{C=O}$ 1689 cm^{-1}; ^1H NMR (CD_3COCD_3) δ 8.17–7.49 (m, 5 H, $-C_6H_5$), 4.88 (s, 2 H, $-CH_2-$), 2.61 (s, 3 H, $-CH_3$), 2.50 (s, 6 H, $-CH_3$), 2.42 (s, 6 H, $-CH_3$), 1.9 (d–t, 6 H, $P(CH_2-)$), 1.47 (m, 12 H, $P(-CH_2-)$), 0.96 (t, 9 H, $P(-CH_3)$, $^3J_{H-H}$ = 6.28 Hz); $^{31}P\{^1H\}$ NMR (CD_3COCD_3) δ 56.7 (s, PBu_3), −142.6 (sp, PF_6, J_{P-F} = 706.4 Hz); MW_{calc} [M^+] 579.2800; M^+_{exp} m/z 579.2799 (Δm = −0.1 mmu).

$\{[\eta^6\text{-}C_6Me_5(CH_2C(O)Ph)]Mn(CO)_2PMe_3\}PF_6$ (4b): light yellow powder; yield, 198 mg (68%) IR (THF) ν_{CO} 1975, 1926 cm^{-1}, $\nu_{C=O}$ 1688 cm^{-1}; ^1H NMR (CD_3COCD_3) δ 8.19–7.61 (m, 5 H, $-C_6H_5$), 4.89 (s, 2 H, $-CH_2-$), 2.60 (s, 6 H, $-CH_3$), 2.40 (s, 9 H, $-CH_3$), 1.69 (d, 9 H, PCH_3, $^2J_{P-H}$ = 8.33 Hz); $^{31}P\{^1H\}$ NMR (CD_3COCD_3) δ 36.99 (s, PMe_3), −141.92 (sp, PF_6, J_{P-F} = 706.7 Hz); MW_{calc} [M^+] 453.1391; M^+_{exp} m/z 453.1394 (Δm = +0.3 mmu). Anal. Calcd (found) for $C_{24}H_{31}O_3P_2F_6Mn$ (**4b**): C, 48.17 (48.24); H, 5.22 (5.12).

$C_6Me_5CH_2C(O)Ph$: white needle crystals; yield, 72 mg (56%); IR (THF) $\nu_{C=O}$ 1680 cm^{-1}; ^1H NMR (CD_3COCD_3) δ 8.16–7.15 (m, 5 H, $-C_6H_5$), 4.54 (s, 2 H, $-CH_2-$), 2.22 (s, 3 H, $-CH_3$), 2.20 (s, 6 H, $-CH_3$), 2.10 (s, 6 H, $-CH_3$).

$\{[\eta^6\text{-}C_6Me_5(CH_2C(O)Ph)]Mn(CO)_2PPh_3\}PF_6$ (4c): yellow powder; yield, 142 mg (82%); IR (THF) ν_{CO} 1981, 1933 cm^{-1}, $\nu_{C=O}$ 1685 cm^{-1}; ^1H NMR (CD_3COCD_3) δ 8.17–7.58 (m, 20 H, $-C_6H_5$), 4.30 (s, 2 H, $-CH_2-$), 2.34 (s, 3 H, $-CH_3$), 2.32 (s, 6 H, $-CH_3$), 2.12 (s, 6 H, $-CH_3$); $^{31}P\{^1H\}$ NMR (CD_3COCD_3) δ 76.16 (s, PPh_3), −142.01 (sp, PF_6, J_{P-F} = 707.2 Hz); MW_{calc} [M^+] 639.1861; M^+_{exp} m/z 639.1853 (Δm = −0.8 mmu).

$\{[\eta^6\text{-}C_6Me_5(CH_2C(O)Ph)]Mn(CO)_2P(OMe)_3\}Cl$ (4d): pale yellow powder; yield, 167 mg (89%); IR (THF) ν_{CO} 1984, 1935 cm^{-1}, $\nu_{C=O}$ 1686 cm^{-1}; ^1H NMR (CD_3COCD_3) δ 8.19–7.51 (m, 5 H, $-C_6H_5$), 4.77 (s, 2 H, $-CH_2-$), 3.40 (br s, 9 H, $P(OCH_3)_3$), 2.51–2.24 (m, 15 H, $-CH_3$); $^{31}P\{^1H\}$ NMR (CD_3COCD_3) δ 196.0 (s, $P(OMe)_3$); MW_{calc} [M^+] 501.1239; M^+_{exp} m/z 501.1248 (Δm = +0.9 mmu).

$\{[\eta^6\text{-}C_6Me_5(CH_2C(O)Ph)]Mn(CO)_2P(OPh)_3\}Cl$ (4e): pale yellow powder; yield, 215 mg (75%); IR (THF) ν_{CO} 1998, 1953 cm^{-1}, $\nu_{C=O}$ 1706 cm^{-1}; ^1H NMR (CD_3COCD_3) δ 8.19–7.59 (m, 5 H, $-C_6H_5$), 7.39–7.23 (m, 15 H, $P(OC_6H_5)_3$), 4.63 (s, 2 H, $-CH_2-$), 2.21 (s, 3 H, $-CH_3$), 2.19 (s, 6 H, $-CH_3$), 2.09 (s, 6 H, $-CH_3$); $^{13}C\{^1H\}$ NMR (CD_3COCD_3) δ 221.27 (CO), 206.25 (C=O), 151.17, 131.33, 130.62 ($-OC_6H_5$), 127.05, 121.96 (ring C), 65.94 ($-CH_2-$), 17.21, 16.81, 15.51 ($-CH_3$); $^{31}P\{^1H\}$ NMR (CD_3COCD_3) δ 159.73 (s, $P(OPh)_3$); MW_{calc} [M^+] 687.1708, M^+_{exp} m/z 687.1698 (Δm = −1.0 mmu).

General Procedure for the Reactions of CH_3I with Complexes 2a–c and 2e. A 100-mL THF solution of a benzyl complex (**2a–c**, **2e**, 0.3–1 mmol) was injected with 40 equiv of iodomethane and stirred for ~5 min. The solution color immediately changed from yellow-orange to yellow. A shift of ν_{CO} in the IR spectra to the higher frequencies of the cationic species indicated reaction completion. The I^- anion was metathesized with 1.1 equiv of NH_4PF_6. The products **5a–c** and **5e** were purified by LC on SiO_2 (hexanes–acetone). Spectroscopic characterizations for the previously unreported compounds follow.

$\{[\eta^6\text{-}C_6Me_5(CH_2CH_3)]Mn(CO)_2P(n\text{-}Bu)_3\}PF_6$ (5a): yield, 256 mg (53%); IR (THF) ν_{CO} 1967, 1918 cm^{-1}; ^1H NMR (CD_3COCD_3) δ 2.89 (q, 2 H, $-CH_2-$, $^3J_{H-H}$ = 7.49 Hz), 2.50 (s, 3 H, $-CH_3$), 2.47–2.46 (m, 12 H, $-CH_3$), 1.88 (d–t, 6 H, $P(CH_2-)$, $^3J_{H-H}$ = 7.0 Hz, $^2J_{P-H}$ = 9.08 Hz), 1.47 (m, 12 H, $P(-CH_2-)$), 1.11 (m, 3 H, $-CH_3$), 0.96 (m, 9 H, $P(-CH_3)$); $^{31}P\{^1H\}$ NMR (CD_3COCD_3) δ 57.4 (s, PBu_3), −142.2 (sp, PF_6, J_{P-F} = 706.3 Hz); MW_{calc} [M^+] 489.2694; M^+_{exp} m/z 489.2685 (Δm = −1.0 mmu). Anal. Calcd (found) for $C_{27}H_{47}O_2P_2F_6Mn$ (**5a**): C, 51.11 (51.18); H, 7.47 (7.32).

$\{[\eta^6\text{-}C_6Me_5(CH_2CH_3)]Mn(CO)_2PMe_3\}PF_6$ (5b): yield, 502 mg (89%); IR (THF): ν_{CO} 1971, 1921 cm^{-1}; ^1H NMR (CD_3COCD_3) δ 2.89 (q, 2 H, $-CH_2-$, $^3J_{H-H}$ = 6.28 Hz), 2.49, 2.46 (br s, 15 H, $-CH_3$), 1.63 (d, 9 H, $P(CH_3)_3$, $^2J_{P-H}$ = 10.01 Hz), 1.22 (t, 3 H, $-CH_3$, $^3J_{H-H}$ = 6.98 Hz); $^{13}C\{^1H\}$ NMR (CD_3COCD_3) δ 225.52 (d, CO, $^3J_{P-C}$ = 25 Hz), 114.81, 114.43, 111.02, 110.68, 110.39, 110.22 (ring C), 24.74 ($-CH_2-$), 19.27 (d, $P(CH_3)_3$, $^3J_{P-C}$ = 30.80 Hz), 17.33, 16.45, 13.50 ($-CH_3$); $^{31}P\{^1H\}$ NMR (CD_3COCD_3) δ 36.40 (s, PMe_3), −141.59 (sp, PF_6, J_{P-F} = 707.1 Hz); MW_{calc} [M^+] 363.1286; M^+_{exp} m/z 363.1287 (Δm = +0.1 mmu).

$\{[\eta^6\text{-}C_6Me_5(CH_2CH_3)]Mn(CO)_2PPh_3\}PF_6$ (5c): yield, 379 mg (55%); IR (THF) ν_{CO} 1976, 1927 cm^{-1}. ^1H NMR (CD_3COCD_3): δ 7.96–7.49 (m, 15 H, $P(C_6H_5)_3$), 2.64 (q, 2 H, $-CH_2-$, $^3J_{H-H}$ = 7.56 Hz), 2.23 (s, 6 H, $-CH_3$), 2.22 (s, 3 H, $-CH_3$), 2.18 (s, 6 H, $-CH_3$), 1.12 (t, 3 H, $-CH_3$, $^3J_{H-H}$ = 7.56 Hz); $^{31}P\{^1H\}$ NMR (CD_3COCD_3) δ 77.26 (s, PPh_3), −142.00 (sp, PF_6, J_{P-F} = 707.2 Hz); MW_{calc} [M^+] 549.1755; M^+_{exp} m/z 549.1766 (Δm = +1.1 mmu).

$\{[\eta^6\text{-}C_6Me_5(CH_2CH_3)]Mn(CO)_2P(OPh)_3\}PF_6$ (5e): yield, 45 mg (65%); IR (THF) ν_{CO} 1995, 1955 cm^{-1}; ^1H NMR (CD_3COCD_3) δ 7.54–7.18 (m, 15 H, $P(OC_6H_5)_3$), 2.85 (br s, 2 H, $-CH_2-$), 2.47, 2.39 (br s, 15 H, $-CH_3$), 1.29 (br s, 3 H, $-CH_3$); $^{31}P\{^1H\}$ NMR

---

(14) IR (THF): **1a** ν_{CO} 1969, 1920 cm^{-1}; **1b** ν_{CO} 1972, 1923 cm^{-1}; **1c** ν_{CO} 1978, 1926 cm^{-1}; **1d** ν_{CO} 1990, 1941 cm^{-1}; **1e** ν_{CO} 1996, 1947 cm^{-1}.

(CD_3COCD_3) δ 172.23 (s, $P(OPh)_3$), −142.65 (sp, PF_6, J_{P-F} = 707.0 Hz); MW_{calc} (M^+) 597.1603; M^+_{exp} m/z 597.1589 (Δm = −1.4 mmu).

Reaction of 2b with CH_3I in the Presence of KH. Iodomethane (200 μL, 3.21 mmol) was added to a THF solution of **2b** (388 mg, 1.114 mmol) and KH (~1 mmol). The progress of the reaction was monitored by IR spectroscopy for 5.5 h. The two products were isolated by column chromatography. The red band eluted first and was identified as $[\eta^6\text{-}C_6Me_5(CH_2CH_3)]Mn(CO)_2I$ by IR and ^1H and $^{31}P\{^1H\}$ NMR spectroscopies. The final yellow band, $[(\eta^6\text{-}C_6Me_{6-n}(CH_2CH_3)_n)Mn(CO)_2PMe_3]I$ (n = 1–3), was isolated as yellow cubic crystals. A 4:3:1 ratio of the three products (n = 1–3) was determined by MS. IR (KBr, THF): ν_{CO} 1972, 1924 cm^{-1}. ^1H NMR (CD_3COCD_3, 298 K): δ 2.89 (m, 3 H, $-CH_2-$), 2.53–2.46 (m, 12 H, $-CH_3$), 1.63 (d, 9 H, $P(CH_3)_3$, J_{P-H} = 10.01 Hz), 1.22 (m, 10 H, $-CH_3$). $^{31}P\{^1H\}$ NMR (CD_3COCD_3): δ 33.8 (s, PMe_3). MW_{calc} [M^+] 363.1286 (n = 1), 377.1442 (n = 2), 391.1599 (n = 3); M^+_{exp} m/z 363.1287 (Δm = +0.1 mmu) (n = 1), 377.1428 (Δm = −1.4 mmu) (n = 2), 391.1593 (Δm = −0.6 mmu) (n = 3).

Reactions of 2d with CH_3I. (a) In THF. Iodomethane (320 μL, 2.73 mmol) was injected into a THF solution of **2d** (142 mg, 358 μmol). The reaction mixture was maintained at 23 °C and monitored by IR spectroscopy for 7.33 h. The only product isolated from the reaction of $[\eta^6\text{-}C_6Me_5(CH_2CH_3)]Mn(CO)_2P(O)(OMe)_2$ (**6**) using LC on SiO_2 (hexanes–acetone–methanol).

(b) In Hexane. The reaction of **2d** (141 mg, 365 μmol) with CH_3I (2.05 mL, 32.9 mmol) produces a 2:3 ratio of **6** to $[\eta^6\text{-}C_6Me_5(CH_2CH_3)]Mn(CO)_2I$ by both IR and ^1H NMR spectroscopics. The products were purified as above.

(c) Catalytic—0.05% CH_3I. A 0.05% CH_3I solution (1.33 μL, 21.4 μmol) in hexane reacted catalytically with **2d** (169 mg, 426 μmol), producing **6** in a 35% recoverable yield. Compound **6** was purified as above.

$[\eta^6\text{-}C_6Me_5(CH_2CH_3)]Mn(CO)_2P(O)(OMe)_2$ (6): yellow powder; yield, 98 mg (51%); IR (THF) ν_{CO} 1964, 1915 cm^{-1}; ^1H NMR (CD_3COCD_3) δ 3.45 (d, 6 H, $P(O)(OCH_3)_2$, $^3J_{P-H}$ = 10.73 Hz), 2.75 (q, 2 H, $-CH_2-$, $^3J_{H-H}$ = 7.66 Hz), 2.34, 2.33, 2.30 (br s, 15 H, $-CH_3$), 1.16 (t, 3 H, $-CH_3$, $^3J_{H-H}$ = 7.55 Hz); $^{13}C\{^1H\}$ NMR (CD_3COCD_3) δ 226.7 (d, CO, $^3J_{P-C}$ = 60 Hz), 112.71, 109.90, 108.98, 108.62 (ring C), 50.27 (d, $P(O)(OCH_3)_2$, $^3J_{P-C}$ = 7.7 Hz), 24.42 ($-CH_2-$), 16.90, 16.10, 13.82 ($-CH_3$); $^{31}P\{^1H\}$ NMR (CD_3COCD_3) δ 137.43 (s, $P(O)(OMe)_2$); MW_{calc} [M^+] 396.0898; M^+_{exp} m/z 396.0904 (Δm = +0.6 mmu).

Kinetic Measurements of the Reaction of CH_3I with Complexes 2a–e. The kinetics were measured over 3–4 half-lives using the intensities of IR carbonyl stretching bands. The reaction solutions were maintained at 25 °C in a mineral oil bath. A ratio of 40:1 iodomethane to "benzyl" complex was used to provide pseudo-first-order conditions. Pseudo-first-order rate constants were calculated from the slope of time versus the log([A]/[A_0]) plots using the SlideWrite*Plus* program. The reaction with **2b** was repeated to demonstrate reproducibility. Complex **2b** was also studied with initial concentration ratios close to 1:1 using iodomethane. A second-order rate constant of $1.5(2) \times 10^{-2}$ $L{\cdot}mol^{-1}{\cdot}s^{-1}$ was obtained for **2b** from a plot of ($[\mathbf{2b}]^{-1} - [\mathbf{2b}]_0^{-1}$) versus time. In each reaction the order for iodomethane and **2b** were both found to be 1.

General Procedure for the Reactions of I_2 with Complexes 2a–e. Solutions of 50 mL of THF and benzyl (**2a–e**, 250–300 μmol) were injected with 3 equiv of iodine and stirred for ~5 min. The solution immediately changed color from yellow-orange to orange. Monitoring of the IR ν_{CO} shifting to the higher frequencies of the cationic species indicated that the reaction was complete. The I^- anion was metathesized with NH_4PF_6 for **2a**, **2b**, and **2d**. The products were purified by LC on SiO_2 (hexanes–acetone). Spectroscopic characterization for the previously unreported compounds follow.

$\{[\eta^6\text{-}C_6Me_5(CH_2I)]Mn(CO)_2P(n\text{-}Bu)_3\}PF_6$ (7a): yield, 182 mg (98%); IR (CH_2Cl_2) ν_{CO} 1975, 1927 cm^{-1}; ^1H NMR (CD_3COCD_3) δ 4.70 (s, 2 H, $-CH_2-$), 2.55 (s, 3 H, $-CH_3$), 2.50 (s, 12 H, $-CH_3$), 1.92 (d–t, 6 H, $P(CH_2-)$, $^3J_{H-H}$ = 7.12 Hz, $^2J_{P-H}$ = 9.01 Hz), 1.49 (m, 12 H, $P(-(CH)_2-)$), 0.96 (t, 9 H, $P(-CH_3)$, $^3J_{H-H}$ = 6.28 Hz); $^{31}P\{^1H\}$ NMR (CD_3COCD_3) δ 56.12 (s, PBu_3), −142.64 (s, PF_6, J_{P-F} = 707.2 Hz); MW_{calc} [M^+] 601.1504; M^+_{exp} m/z 601.1492 (Δm = −1.6 mmu). Anal. Calcd (found) for $C_{26}H_{44}O_2P_2F_6I_1Mn$ (**7a**): C, 41.84 (41.53); H, 5.94 (5.81).

$\{[\eta^6\text{-}C_6Me_5(CH_2I)]Mn(CO)_2PMe_3\}PF_6$ (7b): yield, 207 mg (97%); IR (THF) ν_{CO} 1978, 1930 cm^{-1}; ^1H NMR (CD_3COCD_3) δ 4.71 (s, 2 H, $-CH_2I$), 2.56 (s, 3 H, $-CH_3$), 2.51 (s, 6 H, $-CH_3$), 2.49 (s, 6 H, $-CH_3$), 1.65 (d, 9 H, $P(CH_3)_3$, $^2J_{P-H}$ = 10.16 Hz); $^{13}C\{^1H\}$ NMR (CD_3COCD_3) δ 224.8 (CO), 111.70, 109.12 (ring C), 19.14 (d, PCH_3, J_{P-C} = 31.26 Hz), 17.64, 17.34, 16.39 ($-CH_3$), 1.24 ($-CH_2I$); $^{31}P\{^1H\}$ NMR (CD_3COCD_3) δ 36.37 (s, PMe_3), −142.00 (sp, PF_6, J_{P-F} = 708.0 Hz); MW_{calc} [M^+] 475.0096; M^+_{exp} m/z 475.0106 (Δm = +1.0 mmu).

$\{[\eta^6\text{-}C_6Me_5(CH_2I)]Mn(CO)_2PPh_3\}I$ (7c): yield, 223 mg (84%); IR (THF) ν_{CO} 1982, 1935 cm^{-1}; ^1H NMR (CD_3COCD_3) δ 7.67–7.64, 7.57–7.50 (m, 15 H, $P(C_6H_5)_3$), 4.18 (s, 2 H, $-CH_2I$), 2.30 (s, 9 H, $-CH_3$), 2.21 (s, 6 H, $-CH_3$); $^{31}P\{^1H\}$ NMR (CD_3COCD_3) δ 74.81 (s, PPh_3); MW_{calc} [M^+] 661.0565; M^+_{exp} m/z 661.0569 (Δm = +0.4 mmu).

$\{[\eta^6\text{-}C_6Me_5(CH_2I)]Mn(CO)_2P(OMe)_3\}PF_6$ (7d): yield, 460 mg (75%); IR (THF) ν_{CO} 1996, 1948 cm^{-1}; ^1H NMR (CD_3COCD_3) δ 4.62 (s, 2 H, $-CH_2I$), 3.90 (d, 9 H, $P(OCH_3)_3$, $^3J_{P-H}$ = 9.22 Hz), 2.82 (s, 3 H, $-CH_3$), 2.47 (s, 12 H, $-CH_3$); $^{31}P\{^1H\}$ NMR (CD_3COCD_3) δ 161.74 (s, $P(OMe)_3$), −142.00 (sp, PF_6, J_{P-F} = 707.2 Hz); MW_{calc} [M^+] 522.9943; M^+_{exp} m/z 522.9953 (Δm = +1.0 mmu).

$\{[\eta^6\text{-}C_6Me_5(CH_2I)]Mn(CO)_2P(OPh)_3\}I$ (7e): yield, 85 mg (21%); IR (THF): ν_{CO} 2001, 1957 cm^{-1}; ^1H NMR (CD_3COCD_3) δ 7.43–7.18 (m, 15 H, $P(OC_6H_5)_3$); 4.62 (s, 2 H, $-CH_2I$), 2.58 (s, 3 H, $-CH_3$), 2.53 (s, 6 H, $-CH_3$), 2.48 (s, 6 H, $-CH_3$); $^{31}P\{^1H\}$ NMR (CD_3COCD_3) δ 170.9 (s, $P(OPh)_3$); MW_{calc} [M^+] 709.0413; M^+_{exp} m/z 709.0433 (Δm = +2.0 mmu).

$[\eta^6\text{-}C_6Me_5(CH_2I)]Mn(CO)_2P(O)(OMe)_2$ (8): yield, 40 mg (9%); IR (THF) ν_{CO} 1964, 1918 cm^{-1}; ^1H NMR (CD_3COCD_3) δ 3.84 (d, 6 H, $P(O)(OCH_3)_2$, $^3J_{P-H}$ = 11.90 Hz), 3.62 (vt, 4 H, $-CH_2CH_2I$), 2.79 (s, 6 H, $-CH_3$), 2.57 (s, 3 H, $-CH_3$), 2.53 (s, 6 H, $-CH_3$); $^{31}P\{^1H\}$ NMR (CD_3COCD_3) δ 132.2 (s, $P(O)(OMe)_2$); MW_{calc} [$M + H^+$] 508.9824; M^+_{exp} m/z 508.9805 (Δm = −1.9 mmu).

$\{[\eta^6\text{-}C_6Me_5(CH_2FeCp(CO)_2)]Mn(CO)_2PMe_3\}I$ (9). $FeCp(CO)_2I$ (103 mg, 339 μmol) and **2b** (129 mg, 370 μmol) were combined and solvated with THF. IR (THF): ν_{CO} 2001, 1961, 1950, 1910 cm^{-1}. ^1H NMR (THF-d_8, 213 K): δ 5.29 (s, 5 H, Cp-H), 2.45 (s, 2 H, $-CH_2-$), 2.31, 2.09, 1.68 (s, 17 H, $-CH_3$), 1.44 (d, 9 H, $P(CH_3)_3$, $^2J_{P-H}$ = 8.34 Hz). $^{13}C\{^1H\}$ NMR (THF-d_8, 213 K): δ 226.4 (br s, CO), 110.31, 108.69 (ring C), 86.05 (Cp), 18.39 ($P(CH_3)_3$), 17.58–16.51 ($-CH_3$). $^{31}P\{^1H\}$ NMR (THF-d_8, 213 K): δ 28.15 (s, PMe_3).

$\{[\eta^6\text{-}C_6Me_5(CH_2Mn(CO)_5)]Mn(CO)_2PMe_3\}PF_6$ (10). $Mn(CO)_5Br$ (124 mg, 451 μmol) in ~40 mL of THF was combined with **2b** (149 mg, 428 μmol) in ~50 mL of THF at −55 °C. The reaction mixture was warmed to −45 °C and stirred for 1 h. The resulting bromide salt was metathesized with 1.1 equiv of NH_4PF_6 to give a yellow-orange solid. IR (THF): ν_{CO} 2082, 2045, 2006, 1973, 1928 cm^{-1}. ^1H NMR (THF-d_8, 253 K): δ 2.35 (br s, 5 H, $-CH_2-$, $-CH_3$), 1.98 (br s, 12 H, $-CH_3$), 1.65 (d, 9 H, $P(CH_3)_3$, $^2J_{P-H}$ = 10.24 Hz). $^{13}C\{^1H\}$ NMR (THF-d_8, 253 K): δ 226.1 (s, CO), 222.0, 220.0, 218.4, 212.5 (CO), 131.92 (ring $C\text{-}CH_2-$), 110.73 (ring C), 17.07, 16.81, 16.06, 15.79 ($-CH_3$), −8.0 ($-CH_2-$). $^{31}P\{^1H\}$ NMR (THF-d_8, 253 K): δ 37.56 (s, PMe_3), −141.9 (sp, PF_6, J_{P-F} = 706.9 Hz).

General Procedure for the Reactions of Bu_3SnH with Complexes 2a–e. The benzyl complex (**2a–e**, 150–200 μmol) was mixed with 2.2 equiv of Bu_3SnH in 15–25 mL of dry THF. Immediate color changes from the orange-yellow of the benzyls (**2a–e**) to the pale yellow of the *endo*-$(\eta^5\text{-}C_6Me_6H)Mn(CO)_2PR_3$ complexes (R = n-Bu (**11a**), Me (**11b**), Ph (**11c**), OMe (**11d**), and OPh (**11e**)) were observed. Complete conversion was verified by the presence of only the ν_{CO} of complexes **11a–e** in the IR spectra.[10,15]

---

(15) IR (THF): **11a** ν_{CO} 1908, 1846 cm^{-1}; **11b** ν_{CO} 1910, 1847 cm^{-1}; **11c** ν_{CO} 1913, 1865 cm^{-1}; **11d** ν_{CO} 1924, 1865 cm^{-1}; **11e** ν_{CO} 1941, 1882 cm^{-1}.

General Procedure for the Reactions of $CHBr_3$ with Complexes 2a–e. A 1.1-equiv amount of bromoform was injected into a stirring solution of 50 mL of hexane and benzyl complex (**2a–e**, 200–370 μmol). For each of the phosphine derivatives, a lavender colored precipitate, $[\eta^6\text{-}C_6Me_5(CH_2CHBr_2)]Mn(CO)_2Br$ (**12**), quantitatively formed, leaving the solution clear and colorless. Chromatography of the product removed the eliminated phosphine, detected by odor, and excess bromoform, leaving only **12** as the product for each of the reactions.

$[\eta^6\text{-}C_6Me_5(CH_2CHBr_2)]Mn(CO)_2Br$ (12): IR (THF) ν_{CO} 1975, 1930 cm^{-1}; ^1H NMR (CD_3COCD_3) δ 6.24 (t, 1 H, $-CHBr_2$, $^3J_{H-H}$ = 7.22 Hz), 3.83 (d, 2 H, $-CH_2-$, $^3J_{H-H}$ = 7.28 Hz), 2.44 (s, 6 H, $-CH_3$), 2.29 (s, 9 H, $-CH_3$); MW_{calc} $[C_6Me_5CH_2CHBr_2]$ 335.9739, 333.9757, 331.9775; M_{exp} m/z 335.9738, 333.9751, 331.9782 (Δm = −0.1, −0.6, +0.7 mmu) (2.7%, 5.4%, 2.9%).

General Procedure for the Reactions of CCl_4 or $CDCl_3$ with Complexes 2a and 2b. The chlorocarbon, R′X = CCl_4 or $CDCl_3$, was freshly distilled and deaerated with Ar; and then 40 equiv was added to the benzyl complex (**2a–b**, 250 μmol), forming a red solution. The red solution, $[\eta^6\text{-}C_6Me_5(CH_2CCl_3)]Mn(CO)_2Cl$ (**13**), obtained from reaction of **2b** with CCl_4, typically decomposed within 2–4 h. $[\eta^6\text{-}C_6Me_5(CH_2CDCl_2)]Mn(CO)_2Cl$ (**14**) was obtained as a red solid from the reaction of the benzyls with $CDCl_3$. When exposed to laboratory light, **14** decomposed within 4 h. But **14** was stable in the dark under vacuum or inert atmosphere for over 24 h. Spectroscopic characterizations of the reaction mixtures and products follow.

$[\eta^6\text{-}C_6Me_5(CH_2CCl_3)]Mn(CO)_2Cl$ (13): IR (THF) ν_{CO} 1977, 1931 cm^{-1}; ^1H NMR (C_6D_6) δ 4.10 (br s, 2 H, $-CH_2CCl_3$), 2.19 (br s, 6 H, CH_3), 2.00 (br s, 9 H, CH_3); $^{13}C\{^1H\}$ NMR (C_6D_6) δ 135.1, 134.3, 133.1, 102.1 (ring C), 53.1 ($-CCl_3$), 17.8, 17.6, 17.1, 14.4 ($-CH_3$).

Reaction mixture of 2a + $CDCl_3$: solution exposed to light for ~5 min; $^{31}P\{^1H\}$ NMR ($CDCl_3$) δ 54.09 (s, PBu_3 (**2a**)), 23.14 (s, PBu_3), −32.82 (s, free PBu_3).

Reaction mixture of 2b + $CDCl_3$: solution exposed to light for ~5 min; $^{31}P\{^1H\}$ NMR ($CDCl_3$) δ 36.88 (s, PMe_3 (**2b**)), 11.67 (s, PMe_3), −59.90 (s, free PMe_3).

$[\eta^6\text{-}C_6Me_5(CH_2CDCl_2)]Mn(CO)_2Cl$ (14): IR (THF) ν_{CO} 1975, 1929 cm^{-1}; ^1H NMR ($CDCl_3$) δ 3.54 (br s, 2 H, $-CH_2-$), 2.30 (br s, 6 H, $-CH_3$), 2.19 (br s, 9 H, $-CH_3$); ^2H NMR (THF): δ 4.21 (br s, $-CDCl_2$); $^{13}C\{^1H\}$ NMR ($CDCl_3$): δ 228.7 (CO), 131.9, 106.1, 104.2, 102.0 (ring C), 42.2 ($-CDCl_2$), 16.5, 16.1, 15.8 ($-CH_3$).

X-ray Data Collection, Solution, and Refinement of 2b. Crystals of **2b** were obtained as orange prisms by sublimation under reduced pressure. A summary of the crystal data and refinement parameters is given in Table I. A crystal, 0.39 × 0.15 × 0.12 mm, sealed in a glass capillary tube under dinitrogen, was mounted on the diffractometer. Graphite monochromated Mo Kα radiation, average wavelength = 0.710 73 Å, was used to collect data at 295 K on an Enraf-Nonius CAD4 diffractometer, using an ω scan range, $(0.80 + 0.35 \tan \theta)°$, background at 25% below and above the range; the horizontal aperture was varied from 2.5 to 3.0 mm depending on the angle; the scan speed ranged from 0.71 to 3.3 deg/min for a hemisphere with θ ranging from 1 to 25°. Lorentz, polarization, and empirical absorption corrections were made (μ = 6.9 cm^{-1}, maximum and minimum corrections, 0.97–1.0 on F). Three standards, used to monitor crystal decay, indicated a maximum decline in F^2 of 10.7%; intensity corrections for decay were made. A total of 4163 reflections was measured for the full sphere ($\pm h, \pm k, \pm l$) in reciprocal space for 2θ ranging from 2 to 50°. Averaging 2047 independent reflections greater than 3σ above background gave 1163 reflections that were used in the least-squares refinement. The cell dimensions for the monoclinic crystal, space group $4P2_1/c$, a = 11.967(4) Å, b = 10.093(6) Å, c = 15.232(4) Å, $\alpha = \gamma$ = 90°, β = 102.70(5)°, were obtained by a least-squares fit to 19 orientation reflections in the angle range 10–45° for 2θ.

Table I. Crystallographic Data and Refinement Parameters for $[\eta^5\text{-}C_6Me_5(CH_2)]Mn(CO)_2PMe_3$ (2b)[a]

fw	348.11
cryst dimens, mm	0.39 × 0.15 × 0.12
space group	$P2_1/c$
T, °C	23
a, Å	11.967(4)
b, Å	10.093(6)
c, Å	15.232(4)
β, deg	102.70(5)
V, Å^3	1794.4(8)
Z	4
ρ_{calc}, Mg·m^{-3}	1.556
μ, cm^{-1} (Mo Kα)	7.7
λ, Å (graphite monochromated)	0.710 73
ω scan width, deg	$0.80 + 0.35 \tan \theta$
linear abs coeff, cm^{-1}	7.7
transm coeff	1.00–0.97
data limits, deg	$2 < 2\theta < 50$, ($\pm h, \pm k, \pm l$)
no. of rflns collected	4163
no. of rflns after averaging	2047
no. of rflns > 3σ used in least-squares refinement	1163
no. of params refined	185
R_1[b]	0.059
R_2[c]	0.078

[a] In this and subsequent tables esd's are given in parentheses. [b] $R_1 = \sum ||F_o| - |F_c|| / \sum |F_o|$. [c] $R_2 = [\sum w(|F_o| - |F_c|)^2 / \sum w|F_o|^2]^{1/2}$, $w = 1/s^2(F)$, where $s^2(F) = s^2(F)' + [(0.07)F]^2$.

Table II. Fractional Coordinates and Isotropic Thermal Parameters for 2b[a]

atom	x	y	z	B_{iso}[b] (Å^2)
Mn	0.2052(2)	0.0486(2)	0.7138(1)	3.24(3)
P	0.2036(3)	0.2578(4)	0.6638(3)	5.26(9)
O1	−0.0246(8)	0.001(1)	0.6055(7)	8.2(3)
O2	0.0867(9)	0.122(1)	0.8527(6)	9.4(3)
C1	0.3944(9)	0.047(1)	0.7797(8)	4.2(3)
C2	0.3331(9)	−0.050(1)	0.8151(7)	4.2(3)
C3	0.2635(9)	−0.141(1)	0.7590(7)	3.7(3)
C4	0.2604(9)	−0.134(1)	0.6640(9)	4.5(3)
C5	0.3226(9)	−0.039(1)	0.6312(7)	4.3(3)
C6	0.4165(9)	0.029(1)	0.6910(7)	4.2(3)
C7	0.463(1)	0.149(2)	0.843(1)	6.9(4)
C8	0.338(1)	−0.058(2)	0.9164(8)	6.9(4)
C9	0.200(1)	−0.253(1)	0.794(1)	6.9(4)
C10	0.186(1)	−0.231(2)	0.600(1)	7.3(4)
C11	0.317(1)	−0.028(2)	0.5303(8)	7.9(5)
C12	0.509(1)	0.079(2)	0.668(1)	7.6(5)
C13	0.067(1)	0.020(1)	0.6471(8)	4.4(3)
C14	0.135(1)	0.097(1)	0.7974(6)	4.6(3)
C15	0.082(2)	0.309(2)	0.587(2)	16.5(8)
C16	0.200(3)	0.378(2)	0.749(2)	20.(1)
C17	0.311(2)	0.330(2)	0.621(1)	15.6(7)

[a] Anisotropically refined atoms are given in the form of the isotropic equivalent displacement parameter defined as $(4/3)[a^2B(1,1) + b^2B(2,2) + c^2B(3,3) + ab(\cos \gamma)B(1,2) + ac(\cos \beta)B(1,3) + bc(\cos \alpha)B(2,3)]$. [b] Hydrogen atoms were refined isotropically.

The positions of the manganese and phosphorus atoms were located by Patterson methods. Positional parameters are reported in Table II. Subsequent cycles of least-squares refinement and difference Fourier calculations were used to locate all other non-hydrogen atoms and half the hydrogen atoms, including H12A and H12B on the exocyclic methylene. During the final stages of refinement, the remaining hydrogen atom position were calculated by assigning C–H distances of 0.95 Å and normalizing their positions with respect to located hydrogen atoms. No solvent molecules were found. Anisotropic refinement on all non-hydrogen atoms, except C14 (185 variables, including scale and extinction), gave R values of R_1 = 0.059 and R_2 = 0.078; the standard deviation of an observation of unit weight was 1.28; the maximum parameter shift/estimated error was less than 0.03; the maximum peak height on the final electron density difference map was 0.56 e·Å^{-3}. Weights used in refinement are $1/s^2(F)$, where $s^2(F) = s^2(F)' + [(0.07)F]^2$, and $s^2(F)'$ is the larger of the estimate of the propagated error due to counting error or the estimated error based on agreement of equivalent reflections in the averaging step. The data was processed using scattering factor tables provided in the Enraf-Nonius SDP software package.[16]

Results

A series of (η^5-pentamethylbenzyl)$Mn(CO)_2PR_3$ complexes has been synthesized from the cationic (η^6-hexamethylbenzene)$Mn(CO)_2PR_3$ complexes and characterized. The solid-state structure of **2b** confirms the pentahapticity and the uncoordinated exocyclic double bond in the η^5-cyclohexadienyl ligand. The results of a solid-state structure study undertaken for **2b** are presented in Tables I–III. The structure of **2b**, illustrated in Figure 1, is similar to structures previously found for **2**[5] and **3**.[4d,e] The transformations observed in this work are summarized in Scheme I. Phosphine substitution for a carbonyl on the manganese increases the electron density at the exocyclic methylene, enhancing its nucleophilicity. This is illustrated by comparison of pseudo-first-order rate constants for the reaction of **2a–e** with CH_3I. In the ^1H NMR spectra, coupling of the phosphorus atom to the methylene protons of **2a–b** is observed and the magnitude of this coupling supports arguments for direct interactions between the manganese d_{xy} orbital and the exocyclic methylene. Nucleophilic reactions have been observed to form C–C bonds with CH_3I and PhC(O)Cl and C–I bonds with I_2. Complex **2b** reacts with $Mn(CO)_5Br$ to form $\{[\eta^6\text{-}C_6Me_5(CH_2Mn(CO)_5)]Mn(CO)_2PMe_3\}PF_6$ and with (η^5-C_5H_5)$Fe(CO)_2I$ to form $\{[\eta^6\text{-}C_6Me_5(CH_2Fe(Cp)(CO)_2)]Mn(CO)_2PMe_3\}I$. As well, the benzyls undergo conversion to *endo*-(η^5-C_6Me_6H)$Mn(CO)_2PR_3$ using Bu_3SnH, but not by catalytic hydrogenation. The benzyls can also react by a radical pathway with the halocarbons CCl_4, $CDCl_3$, and $CHBr_3$, to form new C–C bonds at the exocyclic methylene. Observation of a radical species in ESR studies, illustrated in Figure 3, supports the proposed radical mechanism in Scheme II. The details of these results will be discussed at appropriate places in the sections that follow.

Discussion

Synthesis and Characterization of 2a–e. The weak nucleophilic reactivity of **2** at the exocyclic methylene suggests that similar compounds in which a carbonyl is replaced by a stronger σ-donor ligand such as a phosphine ligand could show increased reactivity. The syntheses of **2a–e** were carried out in a 4:1 solution of hexane and THF, which by solubilizing the starting materials, optimizes the formation of the benzyl complexes.[5] In hexane, a nonpolar solvent, KH acts to deprotonate **1a–e**, rather than acting as a hydride nucleophile. Alternate syntheses, using alkyllithium or sodium hydroxide in THF, form the benzyl, but experimental conditions make isolation of the product difficult. Compounds **2b** and **2d** can be purified by sublimation, while **2a**, **2c**, and **2e** decompose at sustained elevated temperatures under reduced pressure. Typically, all the benzyls formed were purified by repeated extraction with hexane to remove them from excess KH. Purity of the products, **2a–e**, was checked by observing the carbonyl bands in the IR spectra, which are distinct from those of the cationic starting materials, **1a–e**, and the cyclohexadienyls, **11a–e**.[10] In the ^1H NMR spectra, **2a–e** each have three characteristic singlet peaks for the inequivalent methyl groups in a 3:6:6 ratio. In the ^1H NMR spectra, the exocyclic methylene protons occur as a singlet for **2c–e** (δ 3.95–3.61) and a doublet for **2a** and **2b** (δ 3.63–3.60). Coupling to phosphorus was verified by observation of a singlet in the $^1H\{^{31}P\}$ spectra. The magnitude of the ^{31}P–^1H coupling (1.2–1.4 Hz) supports involvement of the manganese d_{xy} orbital in a four bond coupling path. The methyl protons of the phosphine in **2b** and **2d** appear as doublets, split by phosphorus, at δ 1.15 and 3.26, respectively. The phenyl protons of both **2c** and **2e** occur between δ 7.73 and 7.38. The butyl groups in **2a** display three proton resonances at δ 1.43, 1.31, and 0.89 for the methylenes adjacent to the phosphorus atom, intervening methylenes, and the terminal methyls, respectively. In the $^{31}P\{^1H\}$ NMR spectra, only the trimethylphosphine derivative, **2b**, deviates substantially from its cationic precursor, **1b**, by shifting upfield by 15 ppm. In each case, only one phosphorus resonance is observed. In the $^{13}C\{^1H\}$ NMR spectra, a peak between δ 233.0 and 228.0 is observed for the CO carbon atoms. Appropriate resonances are observed for the coordinated ring carbon atoms (δ 108.4–76.9) and ring methyl carbon atoms (δ 18.0–15.3). The carbon atoms of the phosphine ligands occur at δ 27.3–12.0 (**2a**), 19.2 (**2b**), 134.1–129.3 (**2c**), 51.9 (**2d**), and 147.1–121.4 (**2e**). The uncoordinated ring carbon atoms appear at δ 145.5 (**2a**), 146.4 (**2b**), 145.0 (**2c**), 148.0 (**2d**), and 152.5 (**2e**) and the exocyclic methylene carbon atom occurs at δ 79.6 (**2a**), 78.8 (**2b**), 79.6 (**2c**), 80.3 (**2d**), and 82.7 (**2e**), closely agreeing with similar assignments for **2**[5] and **3**.[4e] The ^{13}C–^1H coupling constant of 156.5 Hz for the exocyclic methylene of **2d** matches those observed for **2**[5] (158 Hz) and **3**[4e] (156.5 Hz). Because these couplings are virtually the same, they could not provide a suitable measure for potential reactivity of the exocyclic methylene. High resolution EI-MS provided the molecular formulas for compounds **2a–e**, which agree with their proposed structures.

Complexes such as [(η^6-pentamethylbenzene)-$Mn(CO)_2PR_3]PF_6$ (R = Me, OMe) also undergo deprotonation of a ring methyl to form $[\eta^5\text{-}C_6Me_4H(CH_2)]Mn(CO)_2PR_3$ complexes. Gladfelter has recently reported the syntheses of a variety of partially alkylated (η^5-benzyl)$Mn(CO)_3$ complexes, in which the ring has either one or two methyls or one ethyl substituent that has been deprotonated.[6] We isolated the $[\eta^5\text{-}C_6Me_4H(CH_2)]Mn(CO)_2PR_3$ (R = Me, OMe) complexes as a mixture of isomers.[17]

Crystallographic Study of 2b. The crystallographic study was performed to establish the molecular structure of **2b** and to compare it to the published structures of $[\eta^5\text{-}C_6Me_5(CH_2)]Mn(CO)_3$[5] (**2**) and $CpFe[\eta^5C_6Me_5(CH_2)]$[4d,e] (**3**). The solid-state structure of **2b** is illustrated in the ORTEP plot in Figure 1. Selected bond distances and angles are given in Table III. In this "piano stool" structure, the three ligands underneath the (η^5-pentamethylbenzyl)Mn fragment represent the "legs" that are positioned in an

---

(16) Frenz, B. A. *Enraf-Nonius Structure Determination Package*; Enraf-Nonius: College Station, TX, 1981.

(17) $[(\eta^6\text{-}C_6Me_5H)Mn(CO)_2PR_3]PF_6$ (R = Me, OMe), synthesized as in **1a–e**, were deprotonated using the KH procedure described for **2a–e** and were characterized as follows (data for second isomer, if different, in parentheses): (a) Two isomers of $[\eta^5\text{-}C_6Me_4H(CH_2)]Mn(CO)_2PMe_3$ (yellow-orange oil (54%)); IR (THF) ν_{CO} 1926, 1862 cm^{-1}; ^1H NMR (C_6D_6) δ 4.40 (m, 1 H, ring C–H), 3.58 (m, 2 H, $=CH_2$), 1.99 (1.96), (s, 3 H, $-CH_3$), 1.86 (1.84) (s, 3 H, $-CH_3$), 1.79 (1.75) (s, 3 H, $-CH_3$), 1.53 (1.48) (s, 3 H, $-CH_3$), 1.23 (1.16) (d, 9 H, $P(CH_3)_3$, $^2J_{P-H}$ = 8.4 (8.5) Hz). (b) Two isomers of $[\eta^5\text{-}C_6Me_4H(CH_2)]Mn(CO)_2P(OMe)_3$ (yellow-orange oil (62%)); IR (THF) ν_{CO} 1943, 1881 cm^{-1}; ^1H NMR (C_6D_6): δ 4.68 (4.56) (s, 1 H, ring C–H), 3.95 (3.93) (s, 2 H, $=CH_2$), 3.27 (3.26) (d, 9 H, $P(OCH_3)_3$, $^3J_{P-H}$ = 11.0 (10.6) Hz), 2.03 (s, 3 H, $-CH_3$), 1.77 (m, 15 H, $-CH_3$). The balance of the products in both cases was isomers of (η^5-$C_6Me_5H_2$)$Mn(CO)_2PR_3$.

(18) Planes were calculated using the CAD4 Planes programs, Enraf-Nonius; a Table summarizing this data is provided in the supplemental materials.

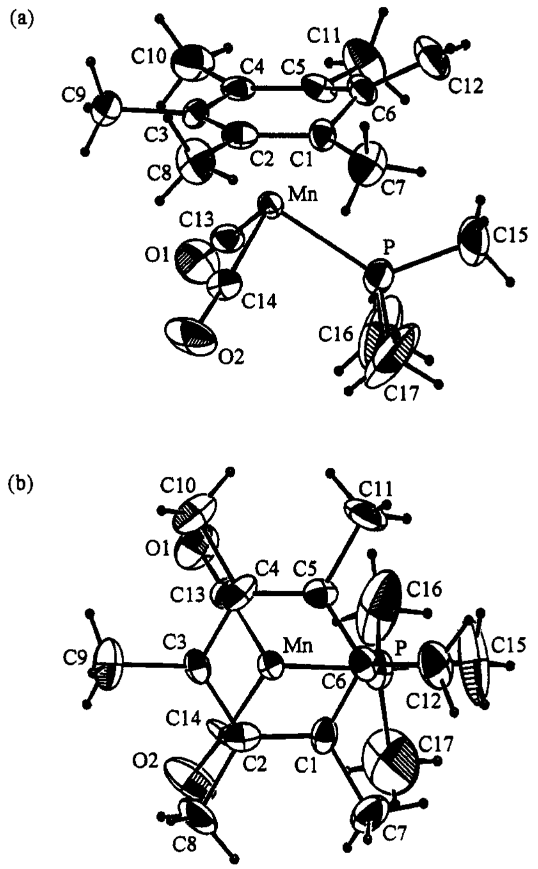

Figure 1. ORTEP drawing of $[\eta^5\text{-}C_6Me_5(CH_2)]Mn(CO)_2PMe_3$ (**2b**) with 25% probability ellipsoids: (a) canted side view and (b) top view.

Table III. Selected Bond Distances (Å) and Angles (deg) for 2b

	Distances		
Mn–C1	2.27(1)	C1–C2	1.403(16)
Mn–C2	2.16(1)	C1–C7	1.516(17)
Mn–C3	2.11(1)	C2–C3	1.401(15)
Mn–C4	2.15(1)	C2–C8	1.534(14)
Mn–C5	2.26(1)	C3–C9	1.519(16)
Mn–P	2.244(3)	C3–C4	1.442(15)
Mn–C13	1.764(13)	C4–C5	1.377(16)
Mn–C14	1.740(11)	C4–C10	1.525(17)
P–C15	1.737(18)	C5–C6	1.453(15)
P–C16	1.782(22)	C5–C11	1.528(14)
P–C17	1.732(16)	C6–C1	1.444(14)
O1–C13	1.157(12)	C6–C12	1.332(16)
O2–C14	1.153(12)		
	Angles		
C13–Mn–C14	85.7(5)	C1–C2–C8	121.0(12)
P–Mn–C13	91.1(4)	C3–C2–C8	117.8(12)
P–Mn–C14	91.0(4)	C2–C3–C4	117.3(9)
Mn–C13–O1	178.1(12)	C2–C3–C9	123.3(12)
Mn–C14–O2	176.8(12)	C4–C3–C9	119.1(12)
Mn–P–C15	116.8(7)	C3–C4–C5	120.2(10)
Mn–P–C16	113.4(7)	C3–C4–C10	119.6(12)
Mn–P–C17	125.1(6)	C5–C4–C10	120.1(12)
C15–P–C17	101.9(11)	C4–C5–C6	120.5(10)
C15–P–C16	97.8(14)	C4–C5–C11	120.6(12)
C16–P–C17	97.1(12)	C6–C5–C11	116.9(11)
C2–C1–C6	119.4(12)	C5–C6–C1	111.7(9)
C6–C1–C7	119.5(11)	C5–C6–C12	126.1(12)
C2–C1–C7	119.1(11)	C1–C6–C12	122.0(12)
C1–C2–C3	121.2(10)		

eclipsed configuration with respect to the ring carbon atoms. The trimethylphosphine ligand is found positioned beneath the exocyclic double bond, where apparently, it experiences the smallest van der Waals repulsion. In *endo*-$(\eta^5\text{-}C_6Me_6H)Mn(CO)_2P(OMe)_3$, the phosphite ligand was found eclipsing the C4 carbon atom rather than beneath the saturated ring carbon atom.[10] In **2b**, the near random positioning of the methyl groups on the phosphine is consistent with free rotation about the Mn–P bond. This causes the anisotropic thermal factors for the phosphine methyl carbon atoms to be twice as large as normal, resulting in increased R values and uncertainties.

The C–C bond distance, 1.33(2) Å, between the unbound ring carbon atom (C6) and the exocyclic methylene carbon atom (C12) is consistent with typical C–C double bonds, matches the bond length found in **2**[5] (1.332(6) Å), and is slightly shorter than that in **3**[4d,e] (1.376(9) Å). The C6 atom is 0.4 Å above the plane formed by the five bound ring carbon atoms,[18] indicating that the benzyl ligand is bound pentahapto rather than hexahapto. The folding dihedral angle, C5/C6/C1 to C1/C2/C3/C4/C5, of the η^5-pentamethylbenzyl ligand is 29(1)°, which is less than that found in **2** (32°) and **3** (32.6°).[4d,e] The folding angles for the η^5-pentamethylbenzyl ligands are well below the typical range for metal-coordinated η^5-cyclohexadienyl ligands (39–50°) which have a saturated uncoordinated ring carbon atom.[10,19,20] On the basis of MO treatments developed by Hoffmann,[20b] Connelly,[21] and Astruc,[22] the folding dihedral angle is dependent upon secondary antibonding interactions between the filled metal d_{xy} orbital and the substituent on the uncoordinated ring carbon atom of the cyclohexadienyl. Thus, it should be anticipated that a smaller dihedral angle is observed with an exocyclic methylene, Figure 2a, compared to an endo alkyl substituent. Furthermore, in the η^5-pentamethylbenzyl ligands, the exocyclic double bond tilts down toward the metal atom. The tilt angle of the C6–C12 bond, relative to the C5/C6/C1 plane, is calculated to be 4.0(2)°, using the displacement of C12 from the C5/C6/C1 plane, −0.092(3) Å, and the C6–C12 bond length. This is about half the tilt angle found in **2**[5] (9°) and **3**[4d,e] (10°). The smaller tilt angle may be attributable to steric interaction with the trimethylphosphine ligand, which has a cone angle of 118°, whereas a carbonyl has a cone angle of 46°.[9] The exocyclic methylene is calculated to be twisted 30° with respect to the C5/C6/C1 plane, using the hydrogen atom positions for H12a and H12b from the Fourier synthesis. Because the twist angle depends on the H12A and H12B positions, the error in the twist angle is uncertain. The twist may be attributed to secondary orbital interaction between the exocyclic π-antibonding orbital (π_a) and the filled metal d_{xy} orbital. The twist may be further stabilized by a symmetry-allowed interaction between the $2\pi_s$ orbital set for the η^5-cyclohexadienyl ring and the π_s orbital of the exocyclic double bond, Figure 2b. The steric demands of the adjacent methyl groups also may contribute to the twist, as was suggested by Astruc for **3**.[4d,22b] The exocyclic CH_2 twist for **2b** lies between the values determined for **2**[5] (38°) and **3**[4d,e] (11°), reflecting the differences in electron donation to the metal orbitals from the CO, PMe_3, and $C_5H_5^-$ ligands.

---

(19) Wilmoth, M. A.; Bernhardt, R. J.; Eyman, D. P.; Huffman, J. C. *Organometallics* **1986**, *5*, 2559–2561.

(20) (a) Hoffmann, R.; Hofmann, P. *J. Am. Chem. Soc.* **1976**, *98*, 598–604. (b) Elian, M.; Hoffmann, R. *Inorg. Chem.* **1975**, *14*, 1058–1076.

(21) Connelly, N. G.; Freeman, M. J.; Orpen, G.; Sheehan, A. R.; Sheridan, J. B.; Sweigart, D. A. *J. Chem. Soc., Dalton Trans.* **1985**, 1019–1026.

(22) (a) Astruc, D. *Synlett* **1991**, 369–380. (b) Green, J. C.; Kelly, M. R.; Payne, M. P.; Seddon, E. A.; Astruc, D.; Hamon, J.-R.; Michaud, P. *Organometallics* **1983**, *2*, 211–218.

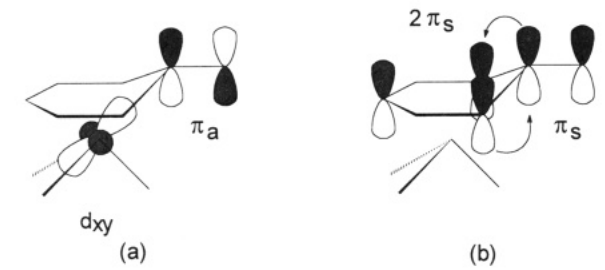

Figure 2. Molecular orbital interactions involving the manganese and cyclohexadienyl-*exo*-ene ligand.

Scheme I

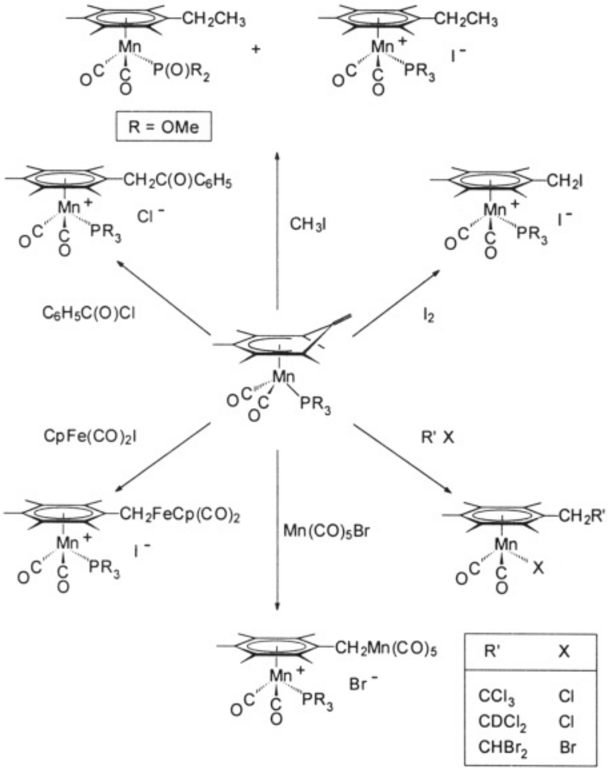

The manganese atom of **2b** may be viewed as occupying a pseudooctahedral environment, with the η^5-pentamethylbenzyl ligand occupying three facial coordination sites. The η^5-pentamethylbenzyl ring is shifted close to the centroid of the C1–C2–C3–C4–C5 crescent to maximize orbital overlap with the π-bonding basis set of the manganese.[20] The Mn–C3 bond length (2.11(1) Å) is the shortest, whereas, the Mn–C5 (2.26(1) Å) and Mn–C1 (2.27(1) Å) bonds are the longest. The constraints imposed by the σ-bonding orbital set require that the tripod of ligands eclipse the C2, C4, and C6 ring carbon atoms.[20] The C13–Mn–C14, P–Mn–C13, and P–Mn–C14 bond angles of 87.7(5), 91.1(4), and 91.0(4)°, respectively, agree with a pseudooctahedral symmetry for the manganese atom.

Reactions of 2a–e. η^5-Pentamethylbenzyl complexes, **2a–e**, have been shown to undergo a diversity of reactions, Scheme I. The coordinated η^5-pentamethylbenzyl ligand is the strong conjugate base of a relatively weak acid, the coordinated η^6-hexamethylbenzene. The exocyclic double bond can be protonated by Brønstead acids to re-form the cationic (η^6-arene)manganese starting compound. This was verified for the title compounds by the addition of NH_4PF_6 (1:1) in THF to protonate **2a–e**. The reaction was observed to proceed quantitatively by IR spectroscopy. The recoverable yield was greater than 95% for each complex. The exocyclic double bonds of the benzyl ligands of **2a–e** react with 2 equiv of Bu_3SnH to form *endo*-(η^5-C_6Me_6H)$Mn(CO)_2PR_3$, **11a–e**. Under catalytic hydrogenation reaction conditions (0.1 g Pd/C (3%), 30 mL of THF, 22.4 mL of H_2, 48 h), the π-carbocyclic ligand is lost and no **11a–e** is observed. The exocyclic double bond can act as a nucleophile or participate in radical reactions with organic halides.[5]

Nucleophilic Reactions of 2a–e. The nucleophilic properties of the exocyclic double bonds of **2a–e** are demonstrated by the formation of C–C, C–I, C–Fe, and C–Mn bonds. In THF, **2** attacks CS_2 forming the zwitterion [η^6-$C_6Me_5(CH_2CS_2^-)$]$Mn^+(CO)_3$.[23] The absence of an EPR signal suggests that the oxidation state of the manganese is unchanged. The benzyls, **2a–e**, attack iodomethane, benzoyl chloride, and iodine, in either hexane or THF, to yield new C–C and C–I bonds. The electrophilic portion, $E^{\delta+}$, of these polarizable reagents is added to the activated exocyclic double bond of the benzyl, eq 5. As illustrated in eq 5, this reaction probably proceeds as a simple S_N2 reaction. The proposed transition state, depicted without methyl groups in eq 5, shows the filled d_{xy} orbital of the manganese overlapping with the empty p orbital of the C6 carbon atom to stabilize the transition state. The displaced $X^{\delta-}$ becomes the counterion of the new cationic (η^6-arene)manganese complex. The enhanced reactivity of **2a–e** cannot be explained by the ground state alone, wherein the exocyclic double bond lengths in **2** and **2b** are equivalent, while the bond length in **3** is longer. Therefore, it is likely that the enhanced reactivity arises during the formation of the transition state rather than the ground state.

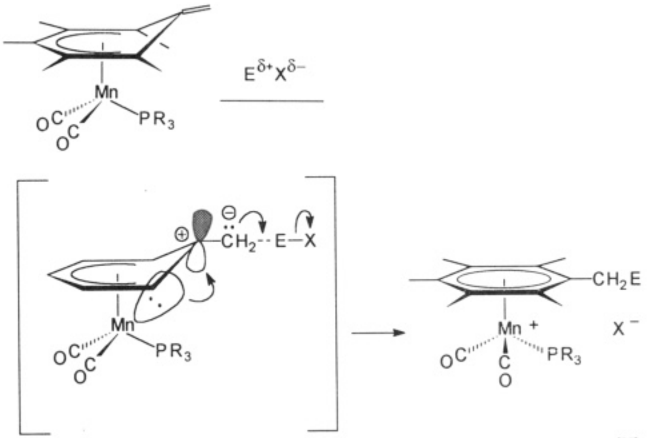

(5)

Compounds **2a–e** were observed to react with benzoyl chloride at rates which are much faster than the rate reported for the tricarbonyl complex, **2**.[5] The rates of reaction for **2c–2e** were slower than for **2a** and **2b**. In all cases, the reactions went quantitatively to **4a–e**, as determined by IR spectroscopy. The IR spectra of **4a–c** and **4e** displayed carbonyl stretches that are 2–3 cm^{-1} higher than those of the starting compounds **1a–1c** and **1e**, while that of **4d** was lower by 6 cm^{-1}; all of which are in the characteristic range observed for terminal carbonyls of cationic (η^6-arene)manganese complexes. The newly formed ketone carbonyl band for these products appears between 1706 and 1685 cm^{-1}. The products were purified by chromatography as the chloride or metathe-

---

[23] LaBrush, D. L. Ph.D. Thesis, University of Iowa, 1989.

sized with NH_4PF_6 in acetone. The products, **4a–e**, were characterized by ^1H and $^{31}P\{^1H\}$ NMR spectroscopy and high resolution FAB mass spectrometry using a 3-NBA matrix. The $-CH_2C(O)-$ protons appear between δ 4.30 and 3.89. The retention of the phosphine ligand in the coordination sphere of the manganese was confirmed by observation of their characteristic proton resonances in the ^1H NMR spectra. Their $^{31}P\{^1H\}$ NMR spectra each contained a single peak for the respective phosphine ligands. The molecular ions of **4a–e**, $[(\eta^6\text{-arene})Mn(CO)_2PR_3]^+$, were observed in HR-FAB MS, verifying their molecular formulas.

The reactions of **2a–e** with both iodomethane and iodine further substantiate the nucleophilic character of the η^5-pentamethylbenzyl ligand. For CH_3I, the alkyl fragment is added to the exocyclic methylene and I^- becomes the counterion. The pseudo-first-order rate constants, k, calculated for the reaction of **2a–e** with excess CH_3I are listed in Table IV. As the electronic contribution from the phosphine ligand increases, k for the methylation reaction increases. For **2b** in THF, a trace amount, less than 2%, of $[\eta^6\text{-}C_6Me_5(CH_2CH_3)]Mn(CO)_2I$ (**19**) forms by way of a competing radical mechanism that will be discussed later. For **2d**, an Arbuzov-like product, **6**, is observed to form exclusively in THF and as a mixture with **19** in hexane. The possibility of the catalytic formation of **6** was verified by the observation that the addition of a catalytic amount of CH_3I (0.05%) to a hexane solution of **2d** yields over 35% of **6**. The remaining compounds, **2a–c** and **2e**, produced the expected nucleophilic reaction products, **5a–c** and **5e**, and only a trace of **19**, anticipated from a radical pathway, was observed during the chromatographic purification of the products. ^1H NMR spectra of **5a–e** displayed a characteristic ethyl group triplet for the methyl (δ 1.22–1.12) and quartet for the methylene (δ 2.89–2.64). In the reaction of I_2 with **2a–e**, I^+ adds to the exocyclic methylene and I^- becomes the counterion. The reaction of **2d** and I_2 produces **8**, an Arbuzov-like product, in small amounts (9%). The ^1H NMR spectra of compounds **7a–e** show the distinctive downfield shift of the $-CH_2I$ protons (δ 4.71–4.18), which is anticipated from the combined field effects of an η^6-arene and iodide substituted on a ring methyl. The $^{31}P\{^1H\}$ NMR spectra of **5a–e** and **7a–e** each contain a single peak for the respective phosphine ligands. HR-FAB MS identified the molecular ions of **5a–e** and **7a–e**, $[(\eta^6\text{-arene})Mn(CO)_2PR_3]^+$, that verify their corresponding molecular formulas.

In the presence of KH, multiple alkylations are observed in the products, $[(\eta^6\text{-}C_6Me_{6-n}Et_n)Mn(CO)_2PMe_3]I$ (n = 1–3), of the reaction of **2b** with excess CH_3I. Reactions of this type, using KH or other bases, have been used by Astruc to produce a variety of "tentacled" arene complexes of iron and cobalt.[24] In our reaction, a minimal amount of KH and only 24 h of reaction time resulted in a maximum of three alkylation attacks on the ring methyls and a product ratio of 4:3:1 (n = 1–3), determined by MS. HR-FAB MS identified the molecular ions of the three products, verifying their corresponding molecular formulas.

Reactions of 2b with $Mn(CO)_5Br$ and $CpFe(CO)_2I$. Compound **2b** reacted with $Mn(CO)_5Br$ at −45 °C to form **10**, an orange product. The carbonyl stretching frequencies observed for the coordinated $-Mn(CO)_5$ are like those obtained by Astruc for $\{CpFe[\eta^6\text{-}C_6Me_5(CH_2Mn(CO)_5)]\}PF_6$.[4d] The ^1H and $^{13}C\{^1H\}$ NMR spectra of **10** display resonances similar to those observed by Astruc. Both IR and NMR spectra confirm the formation of the C–Mn bond at the exocyclic methylene carbon atom. Under similar reaction conditions, $CpFe(CO)_2I$ reacts with **2b** to form **9**. The ν_{CO} shift to higher frequencies suggests the return of the C_6 ring to hexahapto coordination and the addition of the $[CpFe(CO)_2]^+$ moiety to the exocyclic methylene. Corresponding changes in the resonances of the ^1H and $^{13}C\{^1H\}$ NMR spectra and comparison with the spectral results reported by Astruc for $\{CpFe[\eta^6\text{-}C_6Me_5(CH_2Mn(CO)_5)]\}PF_6$ confirm the formation of **9**.[4d]

Radical Reactions of 2a–e. We have proposed a radical mechanism for the reaction with **2** with tetrachloromethane, deuterated chloroform, and bromoform to form complexes of the type $[\eta^6\text{-}C_6Me_5(CH_2CH_nX_{3-n})]Mn(CO)_2X$ (n = 0, 1), shown in Scheme II, using R′X (R′ = CH_nX_{3-n}) as a typical halocarbon.[5] Addition of 9,10-dihydroanthracene (9,10-DHA), a radical inhibitor, slows the rates of these reactions in laboratory light and stops the reaction in the dark after photoinitiation. The phosphine derivatives **2a–e** produce similar products with halocarbon reagents in this process and are influenced in the same way by 9,10-DHA. The proposed initiation of the radical mechanism is the photoinduced dissociation of the phosphine followed by coordination of the halocarbon to the resulting 16-electron manganese species, shown proceeding to the right in Scheme II. Halocarbons coordinated to second and third row transition metals are well documented in the literature.[25] Recent work has established that first row transition metals also coordinate halocarbons.[26] The anticipated weakening of the C-X bond upon coordination in $[\eta^5\text{-}C_6Me_5(CH_2)]Mn(CO)_2(XR')$ (**LD1**), would facilitate homolytic cleavage of the C-X bond to generate $[\eta^5\text{-}C_6Me_5(CH_2)]Mn(CO)_2X^\bullet$ (**LD2**) and $R'^\bullet$ (n = 0, 1) radicals. The possible oxidative addition of R′X to the manganese followed by homolysis of the metal–carbon bond to form the radicals is considered less likely due to steric considerations. However, an alternate initiation process involving electron transfer, shown proceeding to the left in Scheme II, would produce a manganese(II) species (**ET1**) that could react with a $R'^\bullet$

---

(24) (a) Astruc, D. In *Transition Metal Coordination Chemistry*; Dewar, M. J. S., Ed.; Topics in current Chemistry; Springer-Verlag: Berlin, 1991; Vol. 160, pp 63–72. (b) Moulines, F.; Gloaguen, B.; Astruc, D. *Angew. Chem., Int. Ed. Engl.* **1992**, *31*, 458–460. (c) Gloaguen, B.; Astruc, D. *J. Am. Chem. Soc.* **1990**, *112*, 4607–4609. (d) Astruc, D.; Desbois, M.-H.; Lacoste, M.; Moulines, F.; Hamon, J.-R.; Varret, F. *Polyhedron* **1990**, *9*, 2727–2732. (e) Moulines, F.; Astruc, D. *J. Chem. Soc., Chem. Commun.* **1989**, 614–615. (f) Moulines, F.; Astruc, D. *Angew. Chem.* **1988**, *100*, 1394–1396. (g) Hamon, J.-R.; Saillard, J.-Y.; Beuze, A. L.; McGlinchey, M. J.; Astruc, D. *J. Am. Chem. Soc.* **1982**, *104*, 7549–7555.

(25) (a) Laube, T.; Wiedenhaupt, A.; Hunziker, R. *J. Am. Chem. Soc.* **1991**, *113*, 2561–2567. (b) Brown, M.; Waters, J. M. *J. Am. Chem. Soc.* **1991**, *113*, 2442–2443. (c) Colsman, M. R.; Newbound, T. D.; Marshall, L. J.; Noirot, M. D.; Miller, M. M.; Wulfsberg, G. P.; Frye, J. S.; Anderson, O. P.; Strauss, S. H. *J. Am. Chem. Soc.* **1990**, *112*, 2349–2362. (d) Newbound, T. D.; Colsman, M. R.; Miller, M. M.; Wulfsberg, G. P.; Anderson, O. P.; Strauss, S. H. *J. Am. Chem. Soc.* **1989**, *111*, 3762–3764. (e) Winter, C. H.; Veal, W. R.; Garner, C. M.; Arif, A. M.; Gladysz, J. A. *J. Am. Chem. Soc.* **1989**, *111*, 4766–4776. (f) Fernandez, J. M.; Gladysz, J. A. *Organometallics* **1989**, *8*, 207–219. (g) Winter, C. H.; Arif, A. M.; Gladysz, J. A. *Organometallics* **1989**, *8*, 219–225. (h) Barceló, F.; Lahuerta, P.; Ubeda, M. A.; Foces-Foces, C.; Cano, F. H.; Martínez-Ripoll, M. *Organometallics* **1988**, *7*, 584–590. (i) Colsman, M. R.; Noirot, M. D.; Miller, M. M.; Andersen, O. P.; Strauss, S. H. *J. Am. Chem. Soc.* **1988**, *110*, 6886–6888. (j) Winter, C. H.; Gladysz, J. A. *J. Organomet. Chem.* **1988**, *354*, C33–C36. (k) Karipedes, A.; Peiffer, K. *Inorg. Chem.* **1988**, *27*, 3255–56. (l) Kulawiec, R. J.; Crabtree, R. H. *Organometallics* **1988**, *7*, 1891–1893.

(26) Worska, D. C.; Wilson, M.; Bartholomew, J.; Eriks, K.; Prock, A.; Giering, W. P. *Organometallics* **1992**, *11*, 3343–3352.

Scheme II

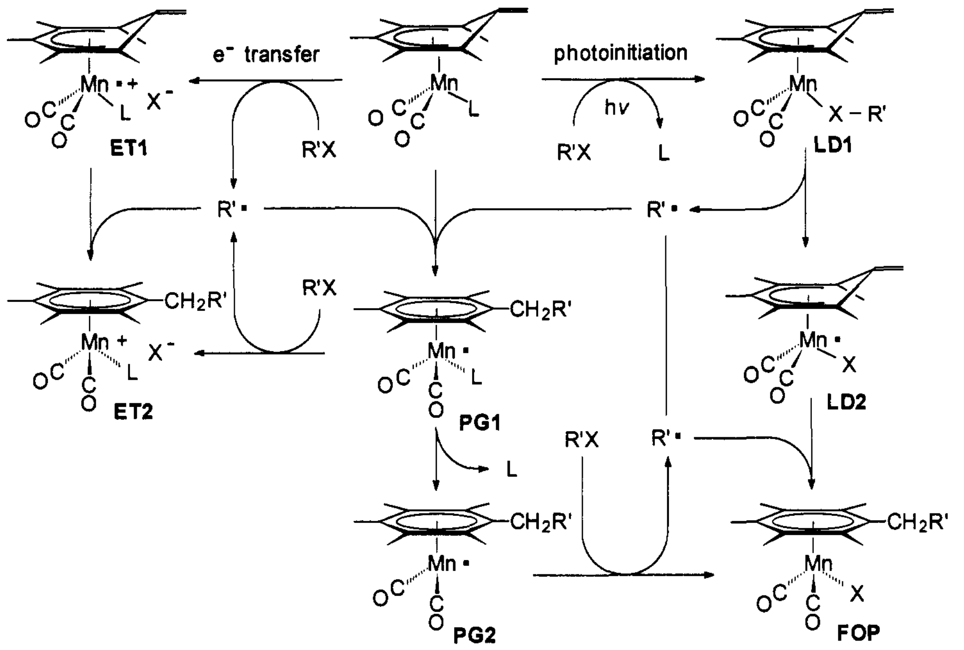

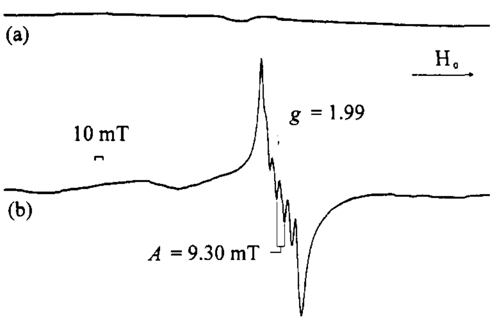

Figure 3. ESR spectra for (a) $[\eta^5\text{-}C_6Me_5(CH_2)]Mn(CO)_2P(n\text{-}Bu)_3$ (**2a**) and (b) **2a** + CCl_4 in THF at 77 K.

to form an (η^6-arene)manganese cation (**ET2**). Formation of **ET1** would be accompanied by generation of R'•.

Formation of the R'• radical serves to initiate a chain mechanism that begins with an attack on a second molecule of **2a–e** at the exocyclic methylene to form the 19-electron $[(\eta^6\text{-arene})Mn(CO)_2L]^\bullet$ (**PG1**) (L = PR_3) radical. The 17-electron species, $[(\eta^6\text{-arene})Mn(CO)_2]^\bullet$ (**PG2**), formed by PR_3 dissociation from **PG1**, abstracts a halogen atom from another R'X, resulting in regeneration of R'•. Reaction of R'• with **LD2** or coupling with another R'• radical furnishes a termination step.

The rates of reaction between a halocarbon and the (η^5-pentamethylbenzyl)manganese complexes are greater when a phosphine is substituted for a carbonyl. This can be partially attributed to the increased lability of the phosphines over a carbonyl in **PG1**. The reaction of **2a–e** with CCl_4 is much faster than with $CDCl_3$, while the reaction of $CHBr_3$ is instantaneous and quantitative in hexane, forming a lavender precipitate, $[\eta^6\text{-}C_6Me_5(CH_2CHBr_2)]Mn(CO)_2Br$.

ESR Studies of the Reactions of 2, 2a, and 2b with CCl_4. ESR spectra of the reactions of **2**, **2a**, and **2b** with CCl_4 provide support for the mechanism proposed in Scheme II. No evidence was found for radicals in the ESR spectra of each of the starting compounds observed as frozen THF glasses at 77 K. The featureless ESR spectrum of diamagnetic **2a** is shown in Figure 3a. A g_{iso} value of 2.192(3) (10% pitch standard) was obtained from the ESR spectrum of **2a** after the addition of CCl_4 at room temperature, followed by transfer to the EPR tube and, immediately thereafter, freezing the solution. Under the same conditions, identical g_{iso} values for **2** and **2b** were obtained. This value is consistent with one unpaired electron on the manganese. The appearance of the ESR spectrum of the reaction mixture of **2a** and CCl_4, Figure 3b, is typical of all three reaction mixtures. The manganese ($I = {}^5/_2$) hyperfine splitting constants, A, for the six-line spectra indicate that the radical species are metal-centered with an A value of 8.6(3) mT for **2**, **2a**, and **2b**. The g_{iso} and A values are consistent with reported cases of one unpaired electron on manganese(II) complexes in an octahedral environment.[27] Typical A values have a reported range of 9.5–5.7 mT. These results suggest that the ESR signal results from **LD2** rather than **PG2**, a manganese(0) species. Hyperfine splitting constants for manganese(0) species have a reported range of 16.7–12.7 mT.[28] The absence of phosphorus hyperfine splitting suggests that the ESR-active species does not have a coordinated phosphorus ligand and therefore must be **LD2** rather than **PG1** or **ET1**.

The $^{31}P\{^1H\}$ NMR spectra of the (**2a** or **2b**) + $CDCl_3$ reaction mixtures each contain three resonances. The first is assigned to the uncoordinated PMe_3 (δ −59.9) or $P(n\text{-}Bu)_3$ (δ −32.8) released during the reaction. The second arises from the coordinated PMe_3 (δ 11.7) or $P(n\text{-}Bu)_3$ (δ 23.1) of a product in which arene is displaced by additional phosphine ligands. The third is assigned to $\{[\eta^6\text{-}C_6Me_5(CH_2CDCl_2)]Mn(CO)_2PR_3\}Cl$ (R = Me (δ 36.9), n-Bu (δ 54.1)), which results from the displacement of Cl^- from the inner-coordination sphere of manganese by phosphine

---

[27] (a) Pike, R. D.; Rieger, A. L.; Rieger, P. H. *J. Chem. Soc., Faraday Trans. 1* **1989**, *85*, 3913–3925. (b) Antanaitis, B. C.; Brown, R. D., III; Chasteen, D.; Freedman, J. H.; Koenig, S. H.; Lilienthal, H. R.; Peisach, J.; Brewer, C. F. *Biochemistry* **1987**, *26*, 7932–7937. (c) Sakurai, H.; Nishida, M.; Yoshimura, T. *Inorg. Chim. Acta* **1982**, *66*, L17–L20. (d) Reed, G. H.; Leyh, T. S. *Biochemistry* **1980**, *19*, 5472–5480. (e) Reed, G. H.; Cohn, M. *J. Biol. Chem.* **1972**, *247*, 3072–3080. (f) Reed, G. H.; Leigh, J. S.; Pearson, J. E. *J. Chem. Phys.* **1971**, *55*, 3311–3316.

[28] (a) Rattinger, G. B.; Belford, R. L.; Walker, H.; Brown, T. L. *Inorg. Chem.* **1989**, *28*, 1059–1066. (b) Wang, S. R.; Cheng, C. P.; Ho, T.-I. *J. Chem. Soc., Dalton Trans.* **1988**, 2695–2699. (c) Ho, T.-I.; Chang, C.-M.; Wang, S. R.; Cheng, C. P. *J. Chem. Soc., Dalton Trans.* **1988**, 123–127.

Table IV. Electrochemical and Rate Data for (η^5-$C_6Me_5CH_2$)Mn(CO)$_2$PR$_3$ Complexes

compd	O_I, $E_{p,a}$[a]	k (s^{-1})[b]	$\nu_{CO}(A_1)$[c]	χ[d]
2a	0.65	1.6(5) × 10^{-3}	1921	1.4
2b	0.67	7.3(4) × 10^{-3}	1924	2.6
2c	0.86	3.3(4) × 10^{-4}	1927	4.3
2d	1.04	1.0(3) × 10^{-4}	1939	7.7
2e	1.20	1.7(3) × 10^{-4}	1955	9.7

[a] $E_{p,a}$ (anodic peak potential), V vs SCE; 0.1 M (n-Bu)$_4$NBF$_4$/THF; sweep rate = 200 mV·s^{-1}; error = ±10 mV; Pt working electrode. [b] Pseudo-first-order rate constants: **2a–e** + $CH_3I \rightarrow$ [(η^6-C_6Me_5Et)Mn(CO)$_2$PR$_3$]I. Reactions observed in THF at 22 °C. Estimated standard deviations are given in parentheses. [c] Infrared symmetric carbonyl stretching frequency observed in THF. [d] Tolman electronic factors for PR$_3$ ligands.[9]

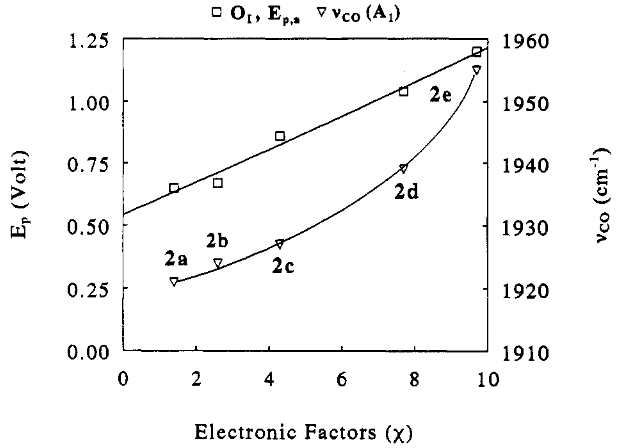

Figure 4. Oxidation potentials (O_I) and symmetric carbonyl stretching frequencies versus the Tolman electronic factors (χ) for [η^5-$C_6Me_5(CH_2)$]Mn(CO)$_2$PR$_3$ complexes.

liberated in the formation of **LD1** and **PG2** in Scheme II. In an independent experiment, the reaction mixture of (η^6-C_6Me_6)Mn(CO)$_2$Cl and an excess of P(n-Bu)$_3$ displayed two of the same ^{31}P resonances as found in the reaction of **2a** and $CDCl_3$, [(η^6-C_6Me_6)Mn(CO)$_2$PR$_3$]Cl (δ 55.0) produced from the chloride displacement and the free P(n-Bu)$_3$ (δ −32.8).

Preliminary UV–visible studies of **2b** and **2d** in hexane displayed little change, upon addition of CCl_4, in the charge transfer bands observed between 240 and 190 nm. The absence of new charge transfer bands supports ligand dissociation rather than electron transfer as the initiation process in the reactions of **2a–e** with CCl_4.

Electrochemical Studies of 2a–e and 2. In order to compare the donor–acceptor properties of the phosphine ligands on the manganese complexes, we have studied the electrochemical properties of **2a–e**. The cyclic voltammetry of **2a–e**, in 0.1 M (n-Bu)$_4$NBF$_4$–THF solution, was performed at a stationary platinum disk electrode at scan rates in the range 200–500 mV·s^{-1} without positive feedback. At a scan rate of 200 mV·s^{-1}, **2a–e** exhibit two oxidation peaks, O_I ($E_{p,a}$ = 0.65–1.20 V vs SCE) (Table IV) and O_{II} ($E_{p,a}$ = 1.36–1.64 V vs SCE), with one reduction peak, R_I ($E_{p,c}$ = −0.81 to −1.16 V vs SCE), being present on the reverse scan.

The first oxidation peak O_I is plotted versus the Tolman electronic factors (χ) for the phosphine and phosphite derivatives, **2a–e**, Figure 4.[9] The symmetric IR stretching frequency for the carbonyls (ν_{CO} (A_1)), another indicator of electron density on the manganese, varies monotonically with χ, Figure 4. Our previous experience with the electrochemistry of *endo*-(η^5-C_6Me_6H)Mn(CO)$_2$PR$_3$ complexes led us to expect a linear correlation between the O_I peak and Tolman electronic factors for the substituted phosphine and phosphite ligands.[10,29] Comparison of O_I values for **2a–e** shows that **2a–c** are more easily oxidized than **2d** and **2e**, consistent with the fact that the phosphites are better π-acceptors or weaker σ-donors than the phosphines.

Peak O_I is chemically irreversible at all scan rates observed, both at 292 and 223 K. The average absolute number of electrons, calculated from the peak areas, approximates a one electron transfer (n = 1.0–1.4), which supports the formation of monoradical cations of **2a–e**, eq 6.

$$2x \rightarrow 2x^+ + e^- \qquad E_{p,a} = 0.65\text{–}1.20\ \text{V} \qquad (6)$$

Peak R_I results from the reduction of the product of the chemical reaction (eq 6) from O_I. This was verified by reversing the scan immediately after traversing O_I and scanning negative to obtain R_I. Peak R_I was not observed without first oxidizing **2a–e**.

Conclusions

We have successfully synthesized and characterized a series of monosubstituted phosphine derivatives of the (η^5-pentamethylbenzyl)manganese tricarbonyl complex. In general, these are more reactive than **2** in nucleophilic and radical reactions because of electronic factors and phosphine ligand lability. The trimethylphosphine derivative, **2b**, extends the chemistry of the manganese complexes to nucleophilic reactions with other organometallic compounds, as Astruc observed for **3**, forming carbon–metal bonds and generating bimetallic complexes. The observed oxidation potentials reflect both the reactivity of the exocyclic methylene and the electron density associated with the various phosphine ligands (alkyl > aryl > alkoxy > aryloxy). The phosphine electron density directly affects the observed rates of the reactions, which increase with stronger σ-donation from the phosphine ligand. Additional support for the radical mechanism in reactions with halocarbons was provided by the presence of manganese centered radical species observed in ESR studies. The solid-state structure of **2b** provides evidence for pentahapto coordination of the benzyl ligand and the presence of the exocyclic methylene and trimethylphosphine ligand. Comparison of the structure of **2b** with the published structures of **2** and **3** reveals the electronic and steric effects which other ligands on the metal induce in the geometry of the benzyl ligand.

The nucleophilicity of the exocyclic methylene is dependent on the electronic environment of the manganese. The phosphine derivatives undergo both nucleophilic and radical reactions, as was observed for **2**. A manuscript in preparation will report (η^5-pentamethylbenzyl)manganese dicarbonyl cyanide derivatives that display a slightly different chemistry.[11] The absence of similar radical intermediates with the cyanide derivatives supports ligand dissociation as an integral part of the initiation process of the reactions of **2a–e** with halocarbons. We are currently extending the chemistry of (η^5-pentamethylbenzyl)manganese compounds by investigating phosphido derivatives.

Acknowledgment is made to the Office of Research and Educational Development at the University of Iowa

---

(29) Snyder, D. B.; Eyman, D. P.; Mundt, D. Unpublished results, The University of Iowa.

for partial support of this research and funds to purchase the VG ZAB-HF mass spectrometer. Accurate mass spectral results from the High Resolution Mass Spectrometry Center at the University of Iowa were obtained by Diane J. Lamb. The Bruker WM-360 NMR spectrometer and the Enraf-Nonius CAD-4 diffractometer were purchased in part with funds from the National Science Foundation (CHE82-01836 and CHE85-07623, respectively). Accurate mass spectral results from the Midwest Center for Mass Spectrometry were partially supported by the National Science Foundation, Biology Division (Grant No. DIR9017262).

Supplementary Material Available: Tables of complete crystallographic and data collection parameters, general displacement parameter expressions, additional bond lengths and angles, hydrogen atoms coordinates, and least-squares planar analysis and an additional ORTEP drawing (6 pages). Ordering information is given on any current masthead page.

OM9300538